CASTOR: The Cosmological Advanced Survey Telescope for Optical and ultraviolet Research

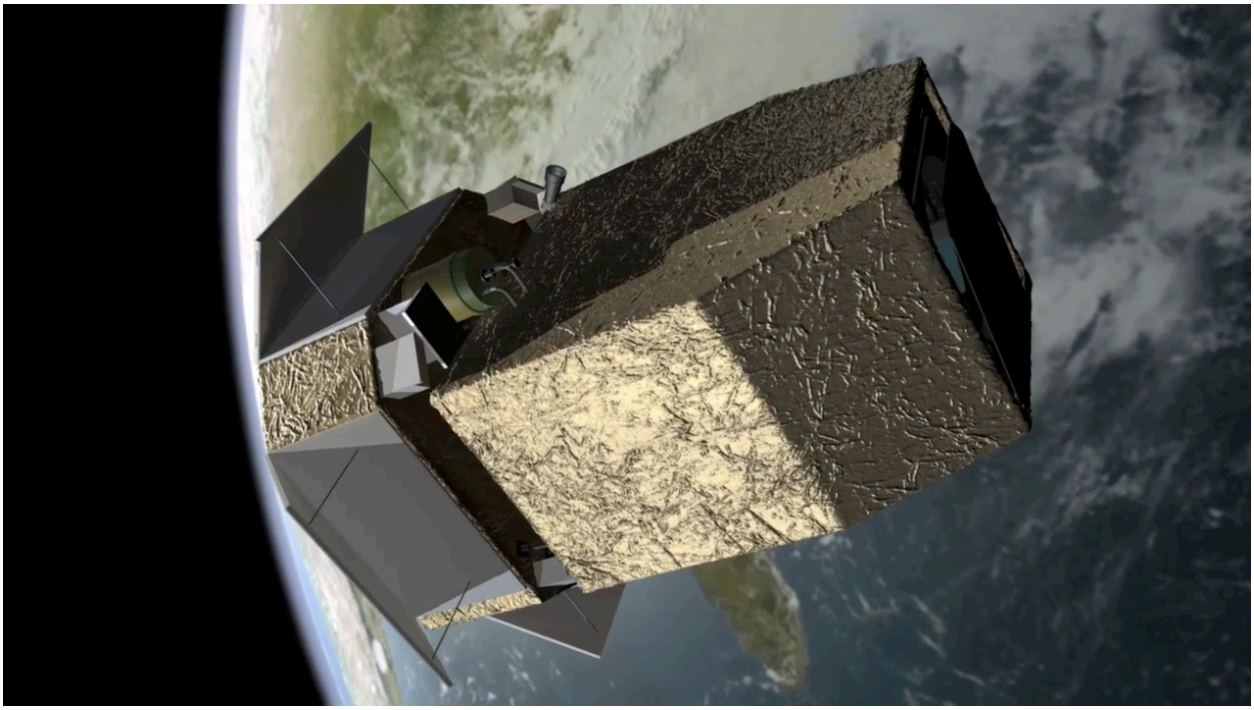

Patrick Côté (NRC), Alan Scott (COM DEV), Michael Balogh (University of Waterloo), Ron Buckingham (Northeast Space), David Aldridge (COM DEV), Ray Carlberg (University of Toronto), Weiguo Chen (COM DEV), Jean Dupuis (CSA), Clinton Evans (COM DEV), Laurent Drissen (Université de Laval), Wes Fraser (NRC), Frederic Grandmont (ABB), Paul Harrison (Magellan), John Hutchings (NRC), JJ Kavelaars (NRC), John-Thomas Landry (ABB), Christian Lange (CSA), Denis Laurin (CSA), Tarun Patel (Magellan), Venka Pillay (Magellan), Louis Piche (COM DEV), Andrew Rader (COM DEV), Carmelle Robert (Université de Laval), Marcin Sawicki (St. Mary's University), Robert Sorba (St. Mary's University), Guillaume Theriault (ABB), Ludovic Van Waerbeke (University of British Columbia)

I. Summary

The Cosmological Advanced Survey Telescope for Optical and UV Research (**CASTOR**) is a proposed CSA mission that would make a unique, powerful, and lasting contribution to astrophysics by providing panoramic, high-resolution imaging in the UV/optical (0.15–0.55 μm) spectral region. This versatile 'smallSAT'-class mission would far surpass any ground-based optical telescope in terms of angular resolution, and would provide ultra-deep imaging in three broad filters to supplement longer-wavelength data from planned international dark energy missions (Euclid, WFIRST) as well as from the ground-based Large Synoptic Survey Telescope (LSST). Combining the largest focal plane ever flown in space, with an innovative optical design that delivers HST-quality images over a field two orders of magnitude larger than Hubble Space Telescope (HST), CASTOR would image about 1/8th of the sky to a (u-band) depth ~1 magnitude fainter than will be possible with LSST even after a decade of operations. No planned or proposed astronomical facility would exceed CASTOR in its potential for discovery at these wavelengths.

II. Mission Context

IIa. Background and Rationale

Wide-field imaging is the backbone of modern astrophysics. Although it has largely been the domain of ground-based telescopes, there is growing recognition within the international astronomical community that many of the most pressing questions in astrophysics and cosmology can only be addressed through wide-field imaging in *space*, which offers a number of key advantages over ground-based observations: i.e., much better image quality and stability, higher observing efficiency, lower sky backgrounds, superior photometric precision, and access to critical spectral regions, such the ultraviolet (UV), that are unobservable from the ground.

Over the past 5-10 years, tremendous international momentum has led to the development of several concepts for a wide-field imaging telescope that would operate in the red-optical through infrared (IR) spectral region (0.55–1.8 μm). The two leading (and competing) missions at this time are **Euclid** (an ESA mission scheduled for launch in 2019) and **WFIRST** (a NASA mission that could launch around 2025). Both missions are motivated primarily by the desire to understand *dark energy* — a mysterious entity that causes an acceleration in the expansion rate of the universe. However, because the legacy value of the proposed imaging is so immense, a vast amount of ancillary science will be enabled by these facilities.

Dark energy missions like Euclid, however, will be compromised without the addition of wide-field imaging at shorter wavelengths: i.e., in the UV and blue-optical region. The expectation at the present time is that these optical data will be provided by ground-based telescopes, most notably by the forthcoming Large Synoptic Survey Telescope (**LSST**). LSST is expected to begin its (decade-long) survey operations around 2020, meaning that the final, stacked images from LSST will therefore not be available until ~2030. Moreover, as a ground-based telescope, LSST will not be able to provide spatial resolution comparable to Euclid, nor will it, of course, include imaging in the critical UV region. Although high-resolution imaging at these UV/optical wavelengths has been possible since the 1990s with the Hubble Space Telescope (HST), this facility lacks the wide field of view needed to survey a significant fraction of the sky, as required by dark energy studies. In any case, HST is approaching the end of its lifetime, with no replacement on the horizon, and will almost certainly have ceased operations by the end of this decade.

This report describes the results of a CSA-sponsored concept study for **CASTOR** (The **C**osmological **A**dvanced **S**urvey **T**elescope for **O**ptical and UV **R**esearch) that was carried out during 2011-2012. This 'smallSAT'-class mission, which could launch as early as 2022, would make a unique, powerful and lasting contribution to astrophysics (and to dark energy studies specifically) by providing panoramic, high-resolution imaging in the UV/optical (0.15–0.55 μm) spectral region (see Figure 1).

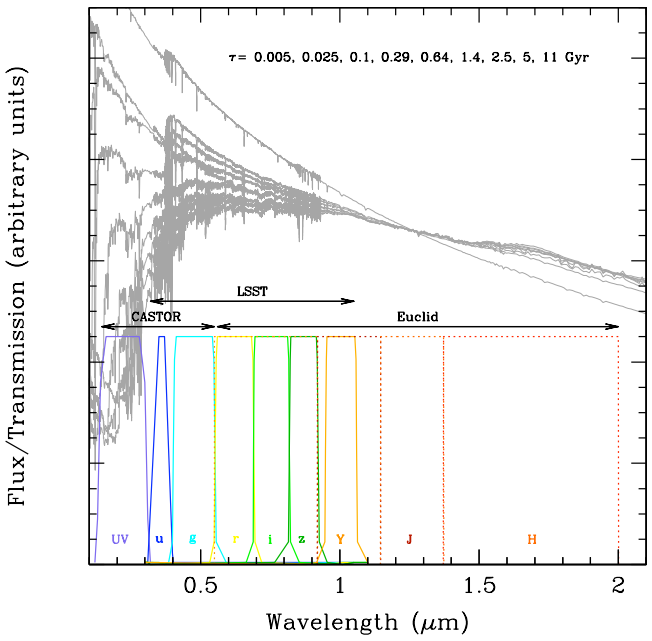

Figure 1: *An illustration of the critical role played by the UV-optical spectral region (0.15-0.55μm) in understanding star and galaxy formation. The grey curves show spectral energy distributions (SEDs) for simple stellar populations (Bruzual & Charlot 2003) having solar metallicity and ages from τ = 5 Myr to 11 Gyr. The SEDs have been normalized at the central wavelength of the J-band, the approximate mean wavelength of the Euclid mission. Note the dramatic variations in the SEDs blueward of 0.5μm, the spectral region for which CASTOR has been optimized, with three filters covering the region 0.15 to 0.55 μm. Planned filters for Euclid (RIZ, Y, J and H) and LSST (u, g, r, i, z, Y) are shown for comparison.*

IIb. Uniqueness and Innovation

No astronomical facility has had a greater impact than the Hubble Space Telescope (HST) which is widely regarded by both scientists and the public as "one of the most productive instruments in the history of science."[1] However, with the fourth and final servicing mission for HST having occurred in 2009, the telescope will almost certainly cease operations before the end of this decade either due to orbit decay or to failure of a critical subsystem (e.g., gyroscopes, batteries). Astronomers worldwide will then soon loose access to the high-resolution, UV/optical imaging capabilities that they have come to rely on for more than two decades — capabilities that have so profoundly changed the astronomical landscape that much of our current understanding of astrophysics and cosmology can be traced directly to HST. NASA's GALEX satellite (Martin et al. 2005), a highly successful SMEX mission that launched in 2003 and pioneered the field of wide-field UV imaging, was defunded by NASA in February 2012.

As discussed below, there is tremendous international momentum behind the development of a new, wide-field space imaging mission. However, the leading candidate at this time (ESA's Euclid satellite) is focused entirely on the red-optical and infrared (IR) region (i.e., 0.55–2.0 μm) where investigations into the nature of dark energy are most efficacious. Yet the effectiveness of Euclid — and of WFIRST, NASA's equivalent dark energy mission — will ultimately hinge on the availability of deep, wide-field optical data to complement the IR imaging. In fact, optical imaging is not only an essential ingredient for dark energy studies, but it is at UV and optical wavelengths that several of the most pressing questions in astrophysics are best addressed (see §III).

According to current plans, the optical data that is required by Euclid will come from 2-8 m-class, ground-based telescopes (e.g., CTIO, Pan-STARRS or LSST), several of which are planning imaging surveys that will cover a few thousand, to tens of thousands, of square degrees over the next 5-20 years. However, placing strong constraints[2] on the nature of dark energy will require optical imaging of truly exquisite quality: i.e., reaching to ultra-faint magnitudes, covering a significant fraction of the sky, and including photometry in the bluest optical bands. These requirements pose a severe challenge for ground-

[1] New York Times Editorial, February 13, 2005.

[2] The ability of individual surveys to constrain the nature of dark energy is usually referred to as the dark energy Figure of Merit (FoM; e.g., Albrecht et al. 2006).

based telescopes. Indeed, wide-field imaging from space offers a number of fundamental advantages compared to ground-based observatories:

Image Sharpness and Atmospheric Turbulence. Before it reaches the ground, light from an astronomical point source must pass through the earth's atmosphere where turbulent mixing blurs the source image into a "seeing disk". Even at the best ground-based sites, the typical *full width at half maximum* (FWHM), which provides a convenient parameterization of the size of this seeing disk, is ≈0.8″. In space, far above the earth's atmosphere, the image quality is, in principle, a function of telescope diameter, D, and wavelength, λ, alone: i.e., the diffraction limit from fundamental physics goes as FWHM ∝ λ/D. The stunning clarity of HST images reflects the fact that HST, though not diffraction limited in the optical, has FWHM ~ 0.1″-0.2″ or about 5-10 times better than the best ground-based telescopes, allowing it to resolve a wealth of detail that is impossible from the ground. While the development of adaptive optic (AO) systems on ground-based telescopes can improve image quality, such gains are typically realized over small fields, only at wavelengths longer than ~0.5 μm, and inevitably come at the cost of a spatially and temporally varying point spread function (PSF; see below).

Access to the Ultraviolet Region. Ground-based telescopes must contend not only with atmospheric turbulence but also with atmospheric absorption. At wavelengths longer than λ~0.8 μm, observations are possible only in discrete, and often narrow, windows (at least until one reaches the broad radio window at ~1 cm), while emission from atoms and molecules in the atmospheric is a further complication at IR wavelengths. Similarly, at wavelengths shorter than ~0.31 μm, the atmosphere is almost entirely opaque due to the combination of ozone absorption and Rayleigh scattering. By contrast, observing from space environments provides unfettered access to this UV region, which is critically important for characterizing emission from young and/or hot sources.

Photometric Calibration and PSF Stability. The photometric precision achieved in astronomical surveys is often limited by systematic errors in the calibration (i.e., changes in system throughput or zero-point, flat-field corrections, etc) and the spatial and temporal stability of the PSF, which characterizes the response of the imaging system to a point source. Unlike ground-based facilities, space telescopes are renowned for their highly stable PSF and photometric calibration.

Low Scattered Light. At ground-based sites, moonlight scattered by the atmosphere will dramatically enhance sky brightness at the shortest wavelengths (i.e., $\lambda \leq 0.6$ μm)where extremely deep imaging from the ground is possible only during periods of low lunar illumination (i.e., dark time). However, even then, atmospheric variations can make accurate photometric calibration difficult. From space, with judicious choices for orbit and pointing strategies, as well as careful telescope baffling, it is possible to capitalize on the extremely dark and uniform skies at short wavelengths.

In short, there are many technical reasons to prefer space environments for wide-field imaging — at both the long- and short-wavelength ends of the UV-optical-IR spectral region. The Euclid and WFIRST missions are being optimized for the long-wavelength end of this spectral region, whereas the CASTOR concept has been developed with the UV and blue-optical regions in mind. Note that the immediate heir to GALEX, the Ultraviolet Imaging Telescope (**UVIT**), is expected to launch in 2013 and will provide astronomers with access to the UV region for a five year period (i.e., until roughly the launch of Euclid at the end of this decade). UVIT will have a somewhat smaller field than GALEX, but improved image quality (FWHM ~ 1.5″). By contrast, CASTOR — with its larger aperture, wider field and far superior resolution compared to UVIT — would offer a dramatic 200-fold gain in point source sensitivity. In any case, no high-resolution UV-optical mission is currently planned by any international space agency beyond ~2020, so CASTOR would plan a key role in space astronomy by filling this important niche.

The power of CASTOR lies in its combination of a wide field with exceptional image quality. Its innovative design is made possible by a compact optical configuration that delivers a wide field at relatively low payload mass. Using state-of-the-art detectors and readout electronics, this enormous field can be covered with a mosaic camera that provides nearly optimal PSF sampling. Although its primary mirror has a relatively modest, 1m aperture, CASTOR will be operate far above the earth's atmosphere and deliver nearly diffraction-limited images (FWHM = 0.15″). This dramatic improvement in spatial resolution compared

to ground-based telescopes (and, even more dramatically, to previous UV imaging telescopes like GALEX) means that CASTOR will exceed even large ground-based imaging telescopes like LSST in terms of depth, and especially, image clarity. For instance, Figure 2 compares the point-source depths as a function of exposure time for CASTOR, LSST, CFHT and GALEX in the UV, u and g bands. For point sources, a 30 min exposure with CASTOR reaches roughly the same depth as LSST after 10 years of operation, but with far superior spatial resolution (see the images in the right panels of Figure 2).

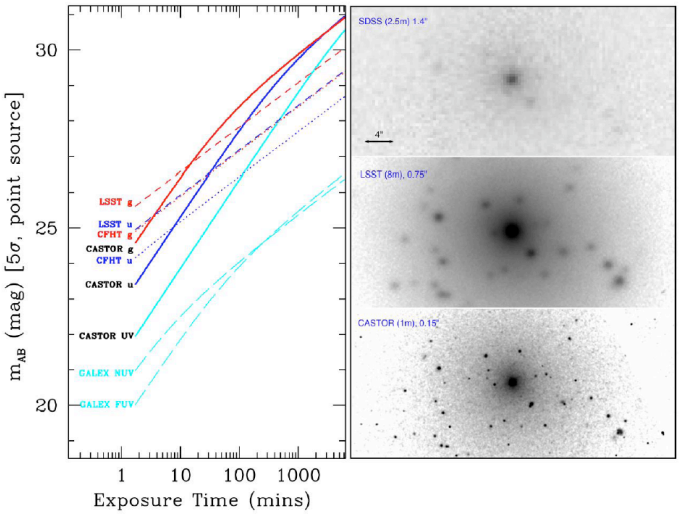

Figure 2: *(Left Panel) Photometric depth as a function of exposure time for CASTOR, CFHT, LSST and GALEX. Results for the UV, u and g bands are shown in cyan, blue and red, respectively. (Right panels) Comparison of g-band images for a typical low-mass galaxy in the Virgo cluster. From top to bottom, these panels show an actual image from the SDSS, and typical images expected from LSST and CASTOR. Despite its modest aperture, CASTOR can provide deeper and far shaper images than is possible with even large ground-based telescopes.*

In short, CASTOR would be a natural successor to HST by far surpassing any ground-based optical telescope in spatial resolution, while dwarfing HST in field of view and providing astronomers with continued access to the critical UV region.

IIc. Operations Model

It is expected that CASTOR will operate with a high level of flexibility, in which the majority of time is initially devoted to carrying out a few Legacy Surveys (see Table 1) and then gradually move into an operations mode that focuses primarily on Guest Observer (GO) programs. Such operational models have recently been adopted with great success by a number of prominent NASA and ESA missions, including GALEX, Spitzer and Herschel.

Table 1. CASTOR Mission Observation Durations

Year	Performance Verification and Calibration	Legacy Surveys	Guest Observer Programs	Targets of Opportunity
1	20%	75%	0%	5%
2	0%	75%	20%	5%
3	0%	50%	45%	5%
4	0%	45%	50%	5%
5+	0%	0%	95%	5%

IId. Synergies with Future Missions and Facilities

There is tremendous interest internationally in the development of a wide-field, high-resolution imaging space telescope. The primary driver for such a facility has been the urgent scientific need to characterize

dark energy, its influence on the evolution of the universe, and its implications for high energy and particle physics. This focus has resulted in the development of both the Euclid (ESA) and WFIRST (NASA) mission concepts. The design and scientific capabilities of these missions are discussed here and are contrasted with the quite different capabilities proposed for CASTOR.

Table 2. Mission Comparisons for WFIRST, Euclid and CASTOR

Mission		WFIRST	Euclid	CASTOR
Lead Agency		NASA	ESA	CSA
Launch		2025+	2018-2019	2022
Telescope Aperture		1.5m	1.2m	1.0m
Telescope Temp.		< 243K	150K (TBC)	280K (ambient)
Focal Plane Temp.		100K	120K/150K	150K
Mission Life		5 years	6 years	5 years
Primary Survey Size		20,000 deg^2	15,000 deg^2	5,000 deg^2
Survey Depth		25.5 AB mag	24.5 AB mag	27.1 AB mag (u)
Visible Imager	Resolution	Combined with NIR (see below)	~0.2″	0.15″
	Sampling		0.1″ per pixel	0.05″ per drizzled pixel
	Wavelength		550 – 920 nm	150 – 550 nm
	# bands		1	3
	IFOV size		0.55 deg^2	0.67 deg^2
	# pixels		25K × 25K	21K × 42K
NIR Imager	Resolution	0.12″ (50% EE)	0.3″	N/A (no capability beyond 1000 nm is envisioned)
	Sampling	0.18″ per pixel	0.3″ per pixel	
	Wavelength	400 – 2000 nm	Y, J, H	
	# bands	5	3	
	IFOV size	0.25 deg^2	0.65 deg^2	
	# pixels	8K × 12K	6K × 6K	
Spectrometer	Type	Slitless	Slitless	Slitless
	Spectral Res.	>75	~500	~100
	Wavelength	1100 – 2000 nm	1000 – 2000 nm	150 – 400 nm
	IFOV size	0.264 deg^2	0.46 deg^2	none
	# pixels	4K × 6K	6K × 6K	TDB

Euclid: Euclid is a medium (M) class ESA mission in the Cosmic Vision 2015-2025 program that is planned for launch from Europe's spaceport at Kourou, French Guiana. The mission itself is the result of the merging of two earlier mission concepts: DUNE (Dark Universe Explorer) and SPACE (SPectroscopic All Sky Cosmic Explorer). The primary goal of the Euclid mission is the study the dark universe using two independent cosmological probes:

- The weak lensing technique which maps the distribution of dark matter and measure the property of dark energy in the universe by measuring the shape distortion of distant galaxy images by intervening large-scale structures. This distortion, or cosmic shear, will be evaluated statistically using a large number of galaxies distributed over an area of 15,000 deg^2 (requirement) to 20,000 deg^2 (goal).
- The baryonic acoustic oscillations (BAO) technique which uses the scales in the spatial and angular power spectra as standard rulers for measuring the equation of state and rate of change of dark energy with redshift. The power spectra will be obtained by measuring with high precision the redshift of a large number of galaxies over the same area used for the weak lensing analysis.

Note that the Euclid design has not been not optimized for studying other dark energy probes (e.g., galaxy clusters or supernovae redshifts). The M-class cost cap (for ESA) is €450M, although the mission will also have contributions from several national space agencies within Europe. The Euclid mission recently completed its definition phase design study and was selected by ESA in October 2011 as one of two M-class missions scheduled for launch in the 2018 to 2019 period.

WFIRST: Since 2007, the US Department of Energy and NASA have been collaborating on a Joint Dark Energy Mission (JDEM) whose main intent was to provide a full order of magnitude improvement in the Dark Energy FoM over anticipated pre-launch dark energy measurements (both from the ground and in space). After intense study by the JDEM Project Office at NASA GSFC during the latter half of 2008 and early 2009, this requirement was deemed incompatible with the $600M cost envelope of medium-class NASA missions. However, the US astronomical community strongly endorsed an observatory-class mission called WFIRST (similar in scope to the JDEM/Omega mission concept) in its US decadal review, where WFIRST was identified as the highest-priority space astronomy project. Despite this strong community support, NASA has indicated that even development work on the WFIRST project could not begin before 2016, due to budget limitations.

The specifications and requirements for Euclid and WFIRST are listed in Table 2 along with the same parameters for the CASTOR mission. Note that the WFIRST parameters are taken from one of the WFIRST candidate missions (JDEM-Omega) while the Euclid parameters are taken from the 2011 Euclid Definition Study Report. The CASTOR parameters listed are those identified as technical requirements by science team in this study.

It is important to emphasize that the capabilities of CASTOR are highly complementary to (and, in many cases, entirely independent of) those of Euclid and WFIRST. As a result, there are significant opportunities for international collaboration on this basis alone. Moreover, many additional scientific studies — over those of the individual missions — would be enabled by a combination of the independent data sets.

III. Science

IIIa. Overview of the Science Investigations

As described in §3.2, the CASTOR has been designed to meet distinct and far ranging scientific goals by virtue of a simple but innovative design and a flexible operations model. A key aspect of CASTOR operations is its ability to conduct ambitious surveys that would answer multiple scientific questions simultaneously (i.e., Legacy Surveys) while still undertaking smaller programs that focus on more specific issues (i.e., Guest Observer, or GO, programs). Table 3-2 summarizes four possible Legacy Surveys, identified by the CASTOR science team, that would guarantee an extraordinary level of scientific impact for the mission. In keeping with the definition of a Legacy Survey, these programs are characterized by their capacity to use a single homogenous data set to investigate key questions in multiple, often distinct, subfields in astrophysics and cosmology.

Wide Survey. The single largest program that is currently envisaged for CASTOR, the Wide Survey would perform "step and stare" imaging over an area of 5000 deg^2, equivalent to roughly 1/8th of the celestial sphere. The key science requirement in terms of survey depth is the need to reach a limiting u-band magnitude of $u_{lim} \approx 27.1$ — roughly one magnitude fainter than the 10-year, stacked-image depth of LSST — to give photometric redshift measurements to the accuracy needed for a reliable characterization of dark energy (once combined with imaging from Euclid and LSST). To ensure a seamless integration of the Euclid, CASTOR and LSST data sets (i.e., to minimize calibration errors), the Wide Survey will be conducted in regions that overlap the Euclid Wide ($b > |30^o|$) and LSST ($\delta < +10^o$) surveys. To reach the requisite u-band depth over the full survey area would require ≈1.8 years of observing time, including overheads. The corresponding depths in the UV and g bands will be $UV_{lim} = 25.8$ and $g_{lim} = 27.8$, respectively. Other key science drivers for the Wide Survey include the history of cosmic star formation, the structure of dark matter halos from weak and strong lensing studies, the mass assembly history of galaxies and their dark matter halos, the outermost structure of the Milky Way, the search of the faintest and most distant objects in the solar systems, and the surface chemistry of small bodies in the Kuiper Belt.

Deep Survey. The Euclid mission aims to carry out RIZ,Y,J,H imaging to a depth of $J_{AB} = 24.5$ over an area of 15,000 deg^2 as well as much deeper imaging to $J_{AB} = 26$ over two, 20 deg^2 fields located close to the northern and southern ecliptic poles. This deep survey, which will allow monitoring of PSF drift through repeated visits at differing orientations over the mission lifetime, will provide exceptionally deep IR images that, when combined with comparably deep UV and optical images from CASTOR, can be used to address a number of fundamental science questions including the faint end of the galaxy (and QSO) mass function and its evolution with redshift, the properties of the oldest and most metal-poor stars in Milky Way, and the nature of the disk-halo transition in the Milky Way. Covering a total area of 40 deg^2 to a depth of $u_{lim} \approx 29.8$ will require ~5 months of observing time, distributed over a period of several years.

Nearby Galaxies Survey. With its exceptional image quality, wide field of view, and UV sensitivity, CASTOR offers a unique opportunity to carry out the definitive imaging survey of galaxies in the local universe. Building on the highly successful *Nearby Galaxies Survey* from GALEX, CASTOR would provide equally wide field coverage, but with a dramatic improvement of ~30 in angular resolution. Pointed observations, requiring ~2 months of observing time, to a u-band depth of 28 (with corresponding UV- and g-band limits of 26.8 and 28.4) would provide unprecedented information on the resolved stellar populations of nearby galaxies. At these depths, it would reach below the horizontal branch, even for the oldest stellar populations, in galaxies at distances up to ~3 Mpc.

Nearby Clusters Survey. Galaxy clusters in the local universe provide invaluable laboratories for studying the fossil record of structure formation in baryonic systems spanning the full range in mass. Contiguous surveys with CASTOR of several "benchmark" clusters in the local universe (most notably the Virgo, Fornax and Coma clusters) would revolutionize the study of the faint end of the galaxy luminosity function, the origin of the most compact stellar systems, the connection between galactic nuclei and super-massive black holes. For the nearby Virgo or Fornax clusters, it will even be possible to study the ages, abundances and spatial distributions of stars filling the intergalactic medium. Observations covering a total area of ~150 deg^2 in these clusters to a depth of $u_{lim} \approx 28$ would require ~ 2 months of observing time.

Full details on the scientific results expected from these Legacy Surveys, and from a number of possible GO programs, may be found in §III. In Figure 3, we show one possible parameterization of the "information content" of astronomical imaging surveys in the UV, optical and IR regions. This figure plots survey depth, *F*, in mJy against Ω/θ, where Ω is total survey area in deg^2 and θ is the FWHM in acrseconds. The location of the CASTOR Wide and Deep Surveys in this figure is shown by the blue symbols. Red symbols show a number of landmark imaging surveys including POSS II, SDSS, 2MASS, CFHTLS, HUDF, GOODS, LSST, and the Euclid Wide and Deep surveys. The dashed diagonal lines indicate factor of 1000 increases in $\Omega/(\theta F)$, meaning that CASTOR will exceed each of the POSS II, SDSS, CFHTLS and GOODS surveys by factors of several thousand in overall information content. In particular, *no planned*

or proposed imaging surveys at these wavelengths will exceed the CASTOR Wide Survey in terms of its potential for discovery.

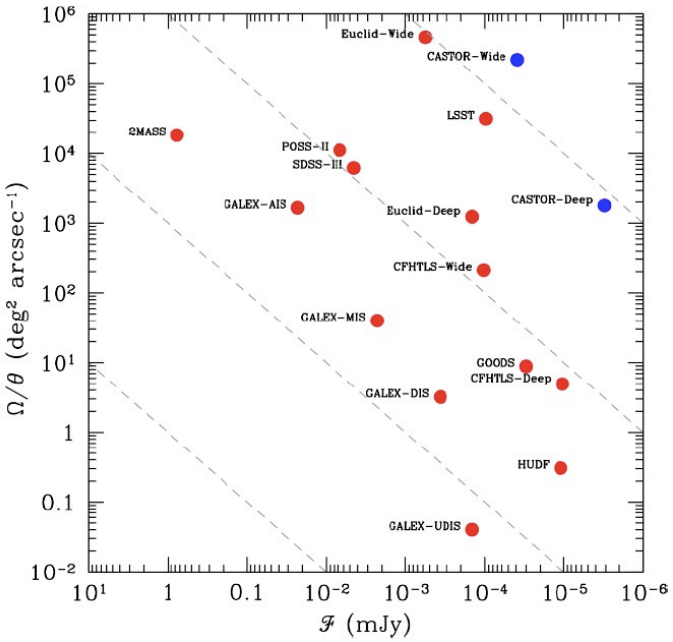

Figure 3: *One representation of the "information content" of wide-field imaging surveys in the UV, optical and IR spectral regions. The abscissa gives the depth, F, of each survey in mJy while the ordinate shows the ratio Ω/θ, where Ω is the survey area in deg² and θ is the FWHM in arcseconds. Information content increases diagonally toward the upper right corner: i.e., dashed lines are separated by factors of a thousand in Ω/θF . Using this metric, the CASTOR Wide and Deep Surveys will each have an information content that is roughly three orders of magnitude greater that of the POSS II, SDSS, GOODS or CFHTLS surveys.*

Table 3. CASTOR Legacy Surveys

Survey	Area (deg²)	Mode	UV_{LIM} (mag)	U_{LIM} (mag)	G_{LIM} (mag)	T (yrs)
Wide	5000	contiguous	25.8	27.8	27.8	1.8
Deep	40	contiguous	29.3	29.8	29.9	0.4
Nearby Galaxies	N≈125	Pointed	26.8	28.0	28.4	0.15
Nearby Clusters	150	contiguous	26.8	28.0	28.4	0.15

IIIb. Investigations and Science Requirements

In this section, we describe a number of primary, or representative, scientific investigations that would be enabled by CASTOR. It is expected that scientific investigations with CASTOR will reflect a balance between four ambitious "Legacy Surveys" and a number of smaller, but more focused, GO programs (see §IIc). Such an operations model requires flexibility in both spacecraft pointing and scheduling. CASTOR has been developed with this flexibility in mind.

1. Dark Energy and Cosmology

Observations carried out over the past decade have firmly established the existence of dark energy, a mysterious form of energy that causes an acceleration in the rate of expansion of the universe. According to current theories, dark energy plays no important role in the *early* universe (e.g., when the cosmic microwave background was generated), but its effects on the expansion become substantial by $z \sim 1$. The primary goal of the next generation of wide-field imaging telescopes is to constrain the nature of dark energy

through a precise measurement of its equation of state as function of redshift.[3] The two key ingredients for such studies are accurate measurements of: (1) galaxy distances from photometric redshifts; and (2) the growth of cosmic structures as a function of time. Because dark energy begins to dominate by $z \sim 1$, it is important to obtain exquisite photometric redshifts and structure growth constraints over the redshift range $0 \leq z \leq 2$. Future wide-field imaging facilities (e.g., Euclid, LSST, Pan-STARRS) are being developed with the expectation that they will work together to provide these constraints. For instance, Euclid has been designed to provide galaxy shapes for gravitational lensing measurements from imaging in a single red-optical (RIZ) filter, as well as photometric redshifts from near-IR imaging. On the ground, LSST and Pan-STARRS are expected to carry out the optical imaging needed to supplement Euclid's near-IR data for the measurement of photometric redshifts.

1.1. *Photometric Redshift Measurements*

The accuracy of photometric redshifts is controlled by both the level of constraints on the gradient of the color terms with redshift, and on the error on the color terms themselves (i.e., the photometric precision). While the latter error can be reduced with deeper observations, the former can only be improved by adding filters over a larger wavelength range (e.g., Benítez 2000; Hildebrandt et al. 2010). This is clearly seen in Figure 4, which compares actual (i.e., spectroscopic) and photometric redshifts for simulated data sets from a variety of planned or proposed imaging surveys (Sorba and Sawicki 2011). In this figure, the Pan-STARRS simulations refer to the final network of four 1.8 m telescopes (i.e., Pan-STARRS-4) while LSST1 and LSST10 refer to LSST imaging after 1 and 10 years of observations, respectively.

The impact of limited wavelength coverage on photometric redshift accuracy (and on catastrophic errors) is immediately apparent. For instance, Euclid alone will provide little useful redshift information (*panel A*). However, once combined with ground-based optical photometry (either from LSST or PanSTARRS), the redshift estimates improve dramatically in quality and reliability. One can see that Euclid+LSST1 (*panel C*) is already superior to Euclid+Pan-STARRS (*panel B*), thanks to the deeper LSST1 data which helps reduce the color gradient error. Combining Euclid and CASTOR imaging (from the Wide Survey) is expected to yield photometric redshifts with precision intermediate to these to cases (*panel E*). Moreover, because photometric redshifts suffer from a fundamental degeneracy between low- and high-redshift galaxies, it can be seen (*panels F* and *G*) that the most precise photometric redshifts are achieved by combining imaging from Euclid, LSST and CASTOR (see also Figure 1). In fact, the redshift range $0 \leq z \leq 1$ is exceptionally clean in this case, thanks largely to the addition of CASTOR photometry. This demonstrates how that the filter set chosen for CASTOR optimally breaks the photometric redshift degeneracies in this critical redshift range. The final redshift precision meets all requirements for an unbiased measurement of the dark energy equation of state based on gravitational lensing data (Albrecht et al. 2006; Huterer et al. 2006), and should ultimately result in sub-percent accuracy in the equation of state parameters w_0 and w_1.

1.2. *The Structure of Dark Matter Halos from Lensing Magnification*

Gravitational lensing based on galaxy shapes is not the only lensing signal one can measure. Lensing also amplifies the total brightness of distant objects in proportion to the amount of foreground mass. This *magnification effect* has recently been detected at relatively high precision in ground-based data sets (Hildebrandt et al. 2009; Hildebrandt et al. 2011) and can be used to probe the mass and structure growth at high redshifts (Van Waerbeke et al. 2010; Van Waerbeke 2010). Magnification has several advantages over the traditional gravitational lensing analysis. Most notably, it requires only photometry (i.e., source galaxies do not have to be resolved) so one can measure lensing to considerably higher redshift than would be possible by measuring shapes alone (which requires the source galaxies to be resolved). Magnification measurements would thus allow the study the dark energy out to redshifts where current theory suggests it was a subdominant component in the energy budget of the universe.

---

[3] The dark energy *equation of state* relates pressure of the universe, P, to its energy density, ρ, through the relation $w = P/\rho$. A widely used parameterization of the equation of state is $w(a) = w_0 + w_1(1-a)$, where a is the scale factor of the universe, w_0 is the equation of state at the present time, and w_1 characterizes the time evolution of the dark energy equation of state.

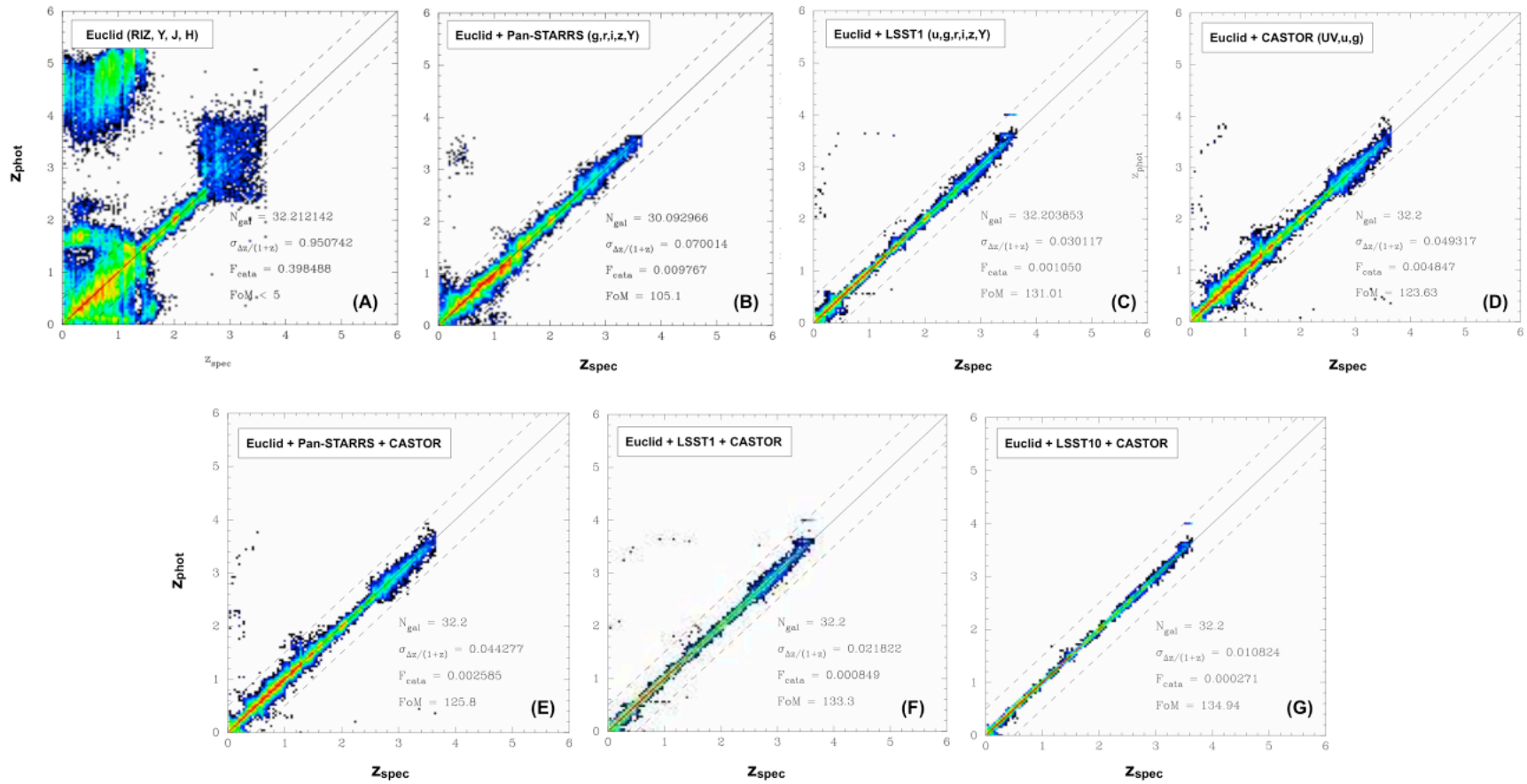

Figure 4: *Comparison of photometric, zphot, and spectroscopic redshifts, zspec, based on seven mock galaxy catalogs that include imaging from the Euclid satellite (see Sorba & Sawicki 2011). Panel (A) shows the comparison for Euclid data alone; Panel (B) shows Euclid plus Pan-STARRS; Panel (C) shows Euclid plus LSST1; Panel (D) shows Euclid + CASTOR; Panel (E) shows Euclid + Pan-STARRS + CASTOR; Panel (F) shows Euclid + LSST1 + CASTOR; and Panel (G) shows Euclid + LSST10 + CASTOR. Note the exceptional level of agreement attained for the combination of Euclid, LSST and CASTOR data, which together fully cover the wavelength range 0.15-2 m. In all panels, Ngal denotes the number of galaxies per square arcminute, σΔz/(1+z) is the overall standard deviation for all galaxies, and Fcata is the fraction of catastrophic redshifts defined by Δz > 0.3 (i.e., the dashed diagonal lines).*

CASTOR will be able to verify this hypothesis and quantify it. The exceptional photometric redshift precision obtained from combining CASTOR with Euclid and LSST — and, in particular, the u and UV bands of CASTOR — will enable the identification of very high redshift star-forming at redshifts $z \sim 2.5$ and higher. These high-z galaxies are ideal source galaxies for magnification measurements (Van Waerbeke et al. 2010; Van Waerbeke 2010) as they would probe dark energy in a redshift range that is completely out of range of Euclid, LSST, PanSTARRS, or any combination of these.

1.3. *High-Redshift Clusters*

Structure growth can also be probed by looking at the abundance of massive, gravitationally bounded objects as function of redshift. This is a well known technique that can be used to set constraints on dark energy (e.g., Vikhlinin et al. 2009). The very precise photometric redshifts from Euclid, LSST and CASTOR (see Figure 4) can be used to identify clusters from a few 10^{13} solar masses to 10^{15} solar masses using matched filter (Milkeraitis et al. 2010), red sequence (Gladders & Yee 2000) or max BCG (Rozo et al. 2010) methods. The CASTOR u and UV bands, combined with longer wavelength data from Euclid and LSST, is ideally positioned for the matched filter approach which offers the advantage of being only weakly dependent on how clusters are precisely defined. Tight constraints on dark energy will then come from the large number of high-z clusters that will be identified with this technique, which can be combined with magnification measurements to place independent limits on the dark energy equation of state over the entire redshift range $0 \leq z \leq 2$ (Van Waerbeke et al. 2010).

1.4. *Cosmic Shear and Galaxy Shapes*

Although Euclid will provide excellent space-based imaging for galaxy shape measurements, there remains some concern that complications could arise from the use of a single, broad, visible filter for the shape measurements. Technically, this complication comes from the fact that stars (which are used to correct the effects of the PSF) do not have the same spectral energy distribution (SED) as galaxies. In other words, one cannot directly use stellar PSFs to correct galaxy shapes, as it is necessary to account for possible *gradient color effects* (Welikala & Kneib 2012). While this problem may be addressed with extensive SED simulations, the narrower u and g filters aboard CASTOR will provide a unique way to explore the gradient color effect directly, on real data, without relying on simulated SEDs. In addition, galaxy shapes from CASTOR measured in the u and g band could help characterize possible systematic errors in the shape measurements at longer wavelengths from Euclid.

2. Galaxy Evolution

Galaxies grow over cosmic time through a combination of *in situ* star formation and hierarchical merging. This evolution can be studied by measuring the growth in stellar mass, the star formation rate (SFR), and the merger rate over wide ranges in cosmic time and environment. The observed evolution must then be linked to the growth in total mass (which is dominated by dark matter) to make robust comparisons with theoretical predictions. By providing wide-field, high-resolution imaging at short wavelengths, CASTOR will allow us to measure the instantaneous *global* star formation rate of galaxies, as well as that of their individual components. We explain below how combining these data with other, complementary surveys will lead to a tremendous step forward in our understanding of galaxy evolution since $z \sim 2$, at a time when the universe was just ~ 3 Gyr old.

2.1. *Evolution of Cosmic Star Formation and Stellar Mass*

The combination of the CASTOR Wide Survey with others at longer wavelengths (e.g., LSST and Euclid) will provide observations spanning the UV to IR for billions of galaxies. Photometric redshifts for galaxies in this sample (see Figure 4) can be measured to a precision of $\Delta z < 0.02(1 + z)$. The observed SEDs can then be fitted with theoretical models to constrain physical parameters. The redder data from LSST and Euclid are critical for establishing the stellar mass and constraining the dust reddening and metallicity. The instantaneous star formation rate (on timescales of ~100 Myr) can be measured from the flux from massive stars, which dominate the SED for $\lambda \leq 0.4$ μm. The UV images from CASTOR will be ideal for measuring this flux for galaxies out to $z \sim 1$. Deep u-band data will serve the same purpose at $1 < z \leq$

1.5. Moreover, the (UV-u) color is a good indicator of dust extinction; together with the LSST/Euclid data, this will allow robust measurements of the intrinsic star formation rate.

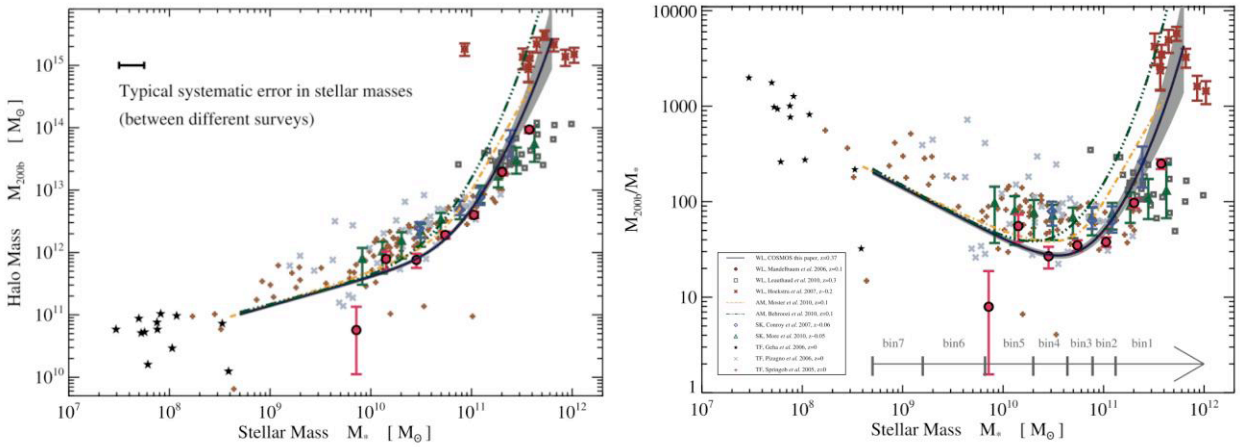

Figure 5: *From Leauthaud et al. (2012), this shows observed constraints on the stellar mass contained within dark matter haloes, as a function of redshift. In principle, this procedure allows astronomers to connect the observed evolution of galaxies with theory. Current work is limited by small sample sizes, cosmic variance and systematic uncertainties due to the need to combine different data sets.*

From these measurements, it will then be possible to measure the stellar mass function and clustering of galaxies with different star formation rates. The clustering analysis provides a measurement of the halo masses, and thus this technique can be used to trace how the connection between halo and stellar mass evolves. A complementary approach will be to stack galaxies (as well as groups and clusters of galaxies) of similar stellar masses and SFRs, and measure their average halo mass from the weak lensing analyses enabled by the Euclid data (and possibly CASTOR as well). Both approaches would allow us to link the growth of stellar mass to the mass assembly history of dark matter haloes, which is now robustly predicted by ΛCDM theory.

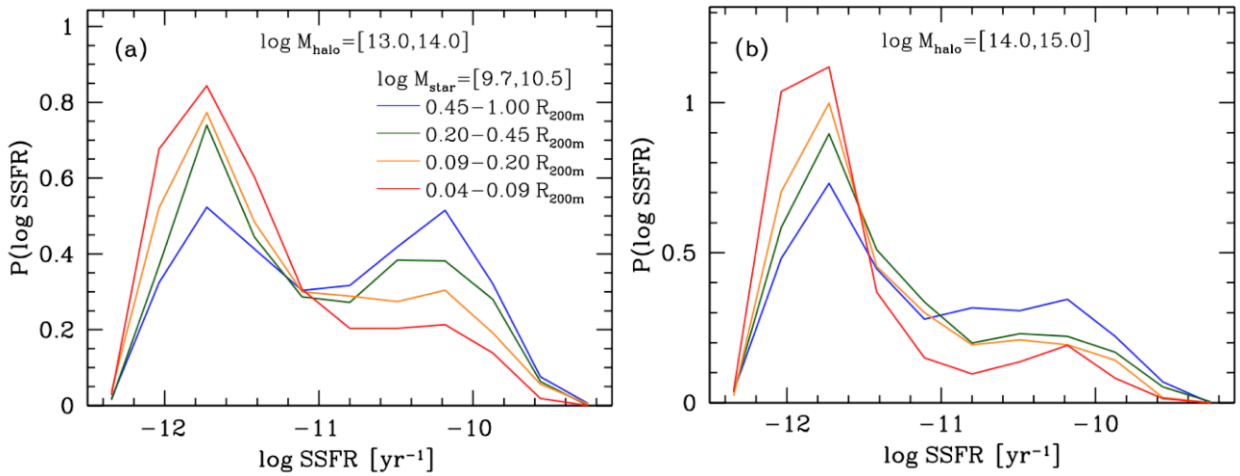

Figure 6: *From Wetzel, Tinker & Conroy (2011), this shows the distribution of SFR/M* at z = 0, for different local environments and halo masses. The analysis is based on SDSS data and shows that the fraction of actively star forming galaxies is strongly dependent on environment. On the other hand, the specific star formation rate of those active galaxies depends only on stellar mass. With CASTOR, it will be possible to improve on this analysis and extend it to z = 2 to map directly the evolution of star formation as it compares with mass assembly.*

Figure 5, taken from Leauthaud et al. (2012), shows the state of the art of this work. While provocative, these results are obtained from small fields and thus statistically limited. Moreover, the results require combining data from different surveys, introducing potentially important systematic uncertainties. The CASTOR Wide Survey will have the statistics and spatial resolution necessary to divide the sample by specific star formation rate and morphology, and thus to disentangle how much of the stellar mass growth is due to *in situ* star formation, and how much is due to merging. It will also allow a measurement of the rate at which star formation is terminated in galaxies, as a function of halo mass and redshift, by comparing the relative growth of the stellar mass function of passive galaxies. This puts important constraints on how star formation and feedback efficiencies, which are currently poorly understood theoretically, are linked to the halo mass of a galaxy.

Supporting data from Euclid and LSST are essential in this case, and the depth of CASTOR data should matched to these surveys so the analysis can be performed on the lowest-mass galaxies possible. Sufficient depth is required to measure galaxies with a wide range of stellar mass over the full redshift range; the star formation density of the Universe has a broad peak at $M > 10^{10.5} M_{\odot}$. The stellar mass limit of the survey will be imposed by the Euclid data, H < 24 (for their wide survey), which corresponds to $M > 2{\times}10^{9} M_{\odot}$ at $z = 1$, and $M > 3{\times}10^{8} M_{\odot}$ at $z = 0.5$. Their proposed deep survey will allow the analysis above to be extended to star-forming galaxies at the 10-year LSST limit of g = 27.4. This extra depth corresponds to a factor ~10 in galaxy mass. We know the rate of galaxy evolution is strongly mass–dependent (e.g., Figure 6), but there exist reliable measurements at these low masses, which is a factor of more than 100 times fainter than probed by the SDSS.

Slitless spectroscopy from CASTOR will be valuable in providing emission-line redshifts for a subset of brighter galaxies. SFR estimates from the [OII] emission line would also be a useful check and constraint for the SED fitting, allowing one to break some important degeneracies in parameter space.

The outcome of a merger depends on the mass ratio of the galaxies, on their orbits, and on their gas content. Thus, while theory robustly predicts the merger rate of dark haloes, the impact of galaxy evolution on major and minor mergers is still controversial. As shown in Hopkins et al. (2010), different models predict significantly different merger rate evolution, but all are roughly consistent with the observational data. Yet these models lead to significant differences in evolution of galaxies, because the mass ratio and gas content of merging pairs is sensitive to the sub-grid physics assumed in many of these models. One of the largest uncertainties here is how stellar content is rearranged following a merger. Some stars are added directly to a spheroidal component from the secondary, while others are transferred from an existing disk in the primary, and still others are formed *in situ* as gas undergoes torques and then flows to the center. Euclid will measure the merger rate of galaxies to unprecedented precision, by resolving close pairs at different stages of interaction, over a wide redshift range. With the UV- and u-band data from CASTOR, it will be possible to measure the SFR of these systems directly, and thus measure how SFR evolves as a merger progresses, and distinguish dynamical growth from growth due to star formation in galaxy bulges.

2.2. *Morphology and Stellar Populations*

CASTOR will also allow a measurement of the *spatially resolved* star formation history of galaxies by employing the same SED-fitting procedure on individual resolution elements (see Figure 7). For example, a typical galaxy at $z \sim 0.5$ will contain >100 independent resolution elements in CASTOR imaging. To reliably measure parameters like the SFR requires S/N > 10 in each, which means the method can be applied for galaxies roughly 2.5 mag brighter than the survey limit. The Deep Survey will thus enable this analysis on galaxies over the same mass range probed globally in the Wide Survey.

The analysis will be less straightforward, but represents a highly unique CASTOR contribution. It will again rely on LSST and, especially, Euclid data of comparable depth. Although LSST images will be of low resolution, those data will be important for measuring a precise redshift for the galaxy. Moreover, the SEDs fitted to the whole galaxy, which will use LSST data, are still important constraints. For example, the average SFR among all independent resolution elements must match the global average for the galaxy. While the CASTOR provides a rest UV-flux measurement for each galaxy, converting this to a SFR requires knowledge of the older stellar population, and dust-reddening in the galaxy; thus the existence of

some high-resolution data at redder wavelengths is essential to robustly measure the SFR. The resolution of Euclid's IR camera is ~0.3″, corresponding to about 25 resolution elements per typical $z \approx 0.5$ galaxy. This is sufficient, at least, to break up the galaxy into broad morphological components (i.e., disk, bulge, bar, nucleus) and to measure the SFR of each component individually. It will then be possible to directly trace the growth of disks, bulges, and bars as a function of cosmic time and environment.

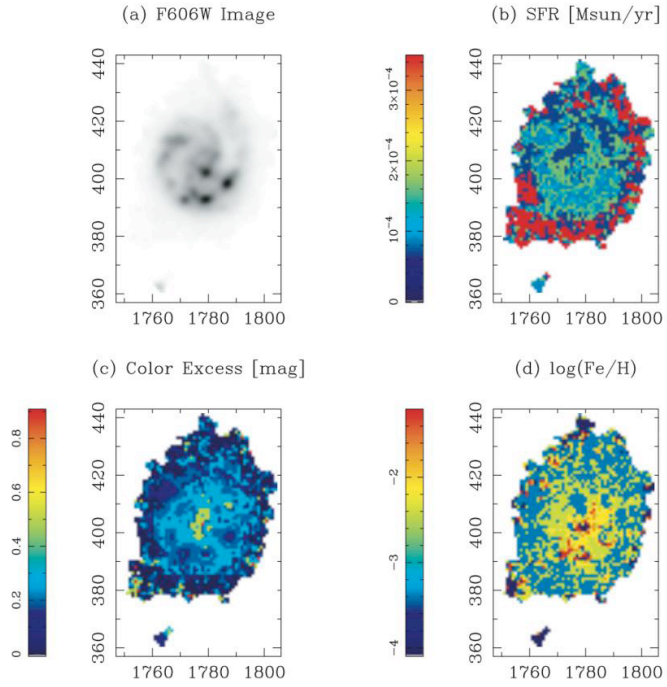

Figure 7: *From Conti et al. (2003). Stellar population synthesis models are used to determine SFR, dust extinction and metallicity for individual pixels within galaxies in the North Hubble Deep Field. CASTOR will be able to make such maps, at slightly lower resolution (FWHM ≈ 0.15″ versus 0.1″ for HST), but for a much larger number of galaxies.*

In fact, CASTOR will be able to measure the SFR on even smaller scales, as its 0.15″ resolution is twice as good as Euclid. Methods to do this need to be developed, but one option would be to use the lower-resolution SED-fits to smoothly model the parameters of mass, dust and metallicity distribution across the galaxy. The rest-UV data can then be used alone, at higher resolution, to map the SFR on sub-kpc scales within individual galaxies. The distribution of star formation, whether ordered (e.g., in spiral arms) or randomly distributed, can be measured as a function of galaxy mass and redshift. This could provide remarkable insights into the modes of star formation and how they are influenced by the mass, redshift or environment of a galaxy.

The central resolution element of a galaxy will be of particular interest, as it can be used to identify the presence of non-thermal (AGN) emission, and thus trace the evolution of these nuclear engines. Moreover, it will enable a measurement of the SFR outside the nucleus, to determine the nature of any correlation between AGN activity and disk-wide star formation.

2.3. *Environments*

Studying the role of environment in galaxy evolution requires imaging over large fields in order to sample a wide range of large-scale environments (i.e., the number of galaxies is not generally a limiting factor in such analyses). The Wide Survey is expected to contain several hundred massive ($M > 5{\times}10^{14} M_{\odot}$) clusters, and tens of thousands of galaxy groups. We know that galaxy evolution is more rapid in these environments, since $z \sim 1$, than in the general population. Although the Deep Survey will not contain many very massive systems, it will still contain about a thousand groups with $M > 10_{14}\ M_{\odot}$. The CASTOR imaging will therefore allow us, for the first time, to determine how that is reflected in the evolution of individual morphological components, especially disks and spiral arms.

The most extreme environments in the universe are the cores of massive galaxy clusters, but these are intrinsically rare and will not be well represented in even the Wide Survey. A dedicated survey of galaxy clusters would be helpful establishing how such clusters assemble, and how they influence galaxy evolution. The ideal survey would cover ~ 100 massive clusters in ~ 5 redshift bins from $z = 0.2$ to $z = 1.5$. This

would require about ~ 1000 hours of survey time. A less ambitious proposal, covering just the most massive clusters, or a more limited redshift range, could be conducted as a GO program.

2.4. *High-Redshift Galaxies*

Deep UV and u images from CASTOR will identify an unprecedented, large population of $z = 2$ galaxies from the well-established Lyman-break selection technique. The wide, uniform imaging will enable a good measurement of the clustering, and hence halo masses, of these galaxies. This will provide an important complement to comparable samples being assembled at $z \sim 3$ and beyond.

2.5. *Dark Matter and Strong Lensing*

Gravitational deflection of light from distant sources by intervening galaxies can form giant arcs, rings and/or multiple images on the scale of arcseconds or less. Such "strong lenses" are important cosmological probes of both galaxy dynamics and the structure of dark matter halos. The most comprehensive searches to date have been based on the SDSS, in which candidate lenses are identified in the SDSS spectroscopic database and then confirmed with high-resolution imaging from HST. The largest SDSS lens survey of this sort has uncovered 85 lenses to date (Auger et al. 2009). Alternatively, wide-field, ground-based imaging can be used to identify candidate lenses having relatively large deflection angles of $\geq 2''$ (i.e., Cabanac et al. 2007). As with searches based on SDSS spectroscopy, follow up imaging with HST is usually required to confirm their nature and to give reliable constraints on the gravitational potential (i.e., mass distribution) of the lensing galaxy.

Recent calculations suggest that LSST, covering an area of ~20000 deg^2, will discover ~6000 strong lensing events to a depth of g ~ 27 mag over a 10-year period. However, with a typical image quality of FWHM ~ 0.75″, interpretation and modeling of these results will be a challenge, as the deflection angles are often comparable to, or smaller than, the seeing disk. By contrast, CASTOR will have far superior image quality than LSST (i.e., by a factor of ~5 in FWHM) making immediate modeling of each system possible. Moreover, the properties of the *source galaxy population* will be much better constrained than will be possible with LSST, thanks to CASTOR's superior u-band depth and angular resolution, and the addition of UV imaging. Scaling the strong lensing predictions for LSST to the area and depth of the CASTOR Wide Survey, we estimate that CASTOR will produce a sample of ~1500 strong lenses with deep 0.15″ images in the UV, u and g bands. With such data, it will be possible to explore the structure of galaxy-scale dark matter halos, and their possible evolution with redshift.

2.6. *Starburst Galaxies*

While not resolving individual stars, CASTOR imaging will provide a quantitative measure of star-formation via the hottest bright stars in galaxies out to redshifts of a few tenths. In rich clusters, these images will show where star-formation is triggered, or quenched by infall from the field. Spectroscopy can then isolate regions of nebular emission associated with star-formation. Combined with stellar population synthesis codes, the SED and nebular emission lines observed can be used to provide information about the star formation rate, age, metallicity, mass, and initial mass function, as well as information about other processes, such as AGN activity and shocks. These properties, which will be obtained easily over the whole surface of the galaxies, are fundamental clues to study galaxy formation and evolution, and represent an important test for theories of stellar evolution.

2.7. *QSOs and Active Galactic Nuclei*

As shown in Figure 8, UV imaging allows QSOs to be selected efficiently in various redshift ranges. Indeed, the CASTOR UV, u and g bands allow high-purity QSO samples to be assembled in the ranges $1 \leq z \leq 2$ and $2 \leq z \leq 4$, with flux alone limiting the selection. Moreover, the angular resolution of CASTOR will make it possible to carry out morphological studies of these QSOs and their nearby companions. At the depth of Wide Survey, it will be possible to identify QSOs with absolute g-band magnitude $M_g \geq -22$ at $z = 4$, and several magnitudes fainter than this at the lowest redshifts (thus reaching deep into the regime of low-luminosity "Seyfert-type" galaxies). This would be the largest and most complete sample of QSOs and AGNs at these redshifts, providing uniquely powerful constraints on QSO evolution. Monitoring of QSOs from repeat observations in the Deep Survey will provide important information on the in-

nermost regions of QSO accretion disks, which are probed directly by their UV and u-band emission; scaling from the GALEX and SDSS surveys, it is expected that Deep Survey observations would yield light curves for ~200,000 QSOs brighter than NUV ≈ 25. Finally, CASTOR slitless spectra for the brightest subset of QSOs identified in the Wide or Deep Surveys would enable definitive classification and verification of the purity of the photometric samples. Statistical studies of the morphology and environment of the QSO samples would provide important information on the environment and triggering of QSO events.

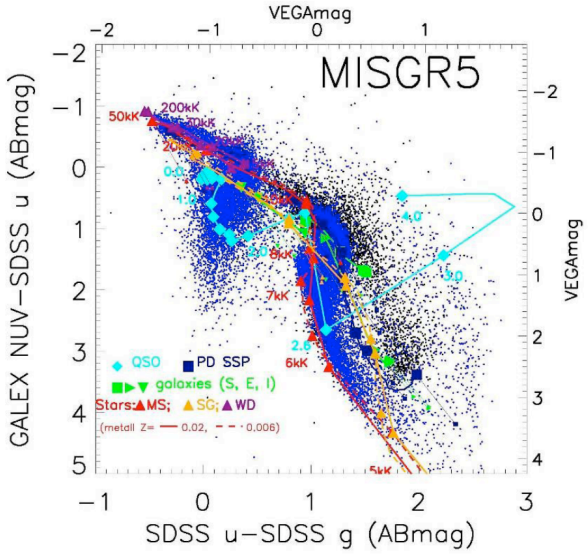

Figure 8: *Color-color diagram showing the distribution of sources observed in the NUV, u, and g bands with GALEX and SDSS. These colors correspond closely to what will available from CASTOR. Blue points show sources that are unresolved in SDSS while black points show extended objects. Note that the central swath of blue points overlies many black points. The cyan track shows typical QSO colors over the range 0 z 4. Other curves show stellar tracks for a range in effective temperature. Vectors indicate 0.3 mag of local reddening.*

3. Near-Field Cosmology

The formation and evolution of the cosmic structures is a complex problem that can be approached in one of two ways: through direct observations of distant objects spanning a range in look-back time, or through *in situ* studies of the "fossil record" imprinted in nearby star clusters, galaxies, groups, and galaxy clusters (i.e., near-field cosmology). This second technique is a burgeoning field that is driving the development of many future facilities (e.g., GAIA, LSST, etc). CASTOR will be a uniquely powerful addition to this array, offering excellent image quality, wide field coverage, and access to the UV and blue-optical spectral regions. In this section, we describe a few examples of near-field cosmology programs that can be undertaken with CASTOR.

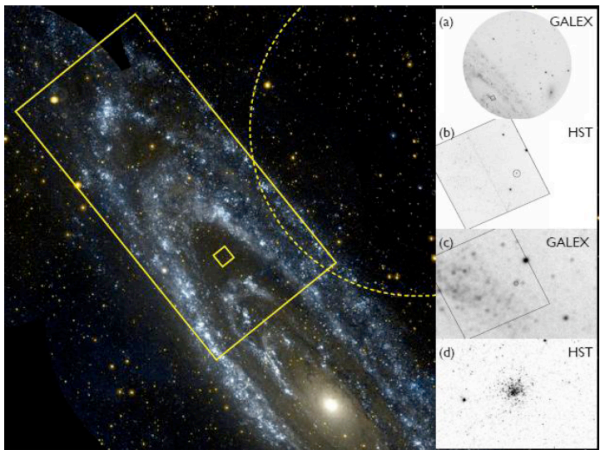

Figure 9: *Demonstration of the power of CASTOR, relative to HST and GALEX, for wide-field, high-resolution imaging of nearby galaxies. The underlying image is a mosaic of M31 constructed from multiple GALEX images. The field of view of a single GALEX image is shown as the dashed circle. The large rectangle shows the CASTOR field of view, which measures 1.16° ×0.58°. The smaller polygon shows the HST/ACS field, which is ~1/200th that of CASTOR. The insets show magnified views from GALEX and HST imaging. CASTOR will have angular resolution comparable to HST, and ~30× better than that of GALEX.*

3.1. *The Star Formation and Accretion Histories of Nearby Galaxies*

As noted in §IIIa, an obvious candidate for a CASTOR Legacy Survey is panoramic UV-, u- and g-band imaging for several hundred nearby galaxies. Such a survey would capitalize on the facility's excellent image quality, wide field coverage, and UV sensitivity. During the last five years, a number of large HST programs (totaling nearly 2000 orbits) have been devoted to imaging surveys of this sort (though with limited areal coverage). Meanwhile, GALEX carried out a highly successful UV imaging survey of several hundred nearby galaxies soon after its launch in 2003. Compared to these studies, CASTOR would provide an unparalleled view of the stellar content in nearby galaxies thanks to a ~200-fold increase in field size compared to HST/ACS, and a ~30-fold improvement in FWHM compared to GALEX (Figure 9). Crowding in these galaxies makes studying their resolved stellar populations with ground-based telescopes (e.g., LSST or Pan-STARRs) virtually impossible for all but the nearest systems. Furthermore, ground-based facilities cannot probe the critical UV region, where the emission from young stars is largest. Figure 10 shows how CASTOR imaging could map out the history of star formation in nearby galaxies with panoramic, UV/optical imaging having HST-like resolution.

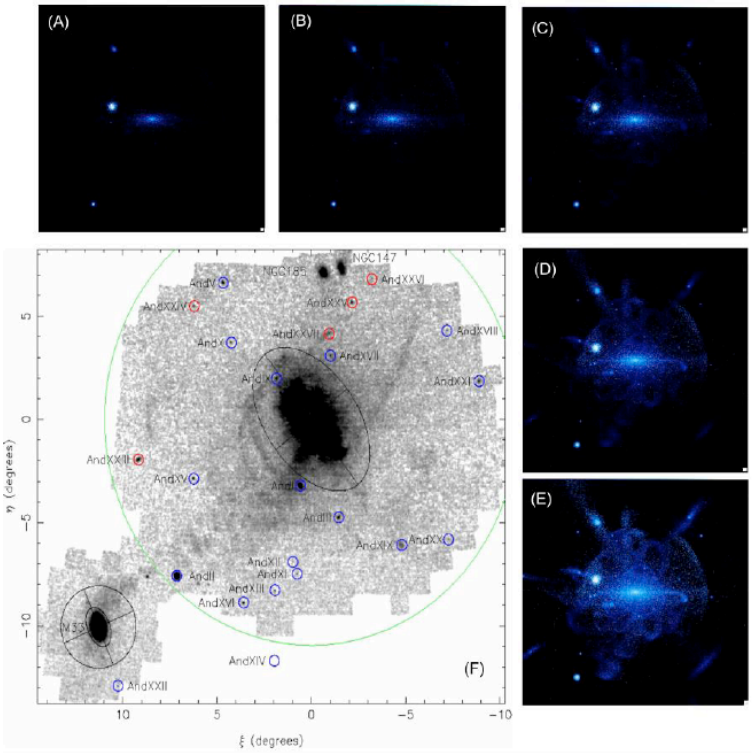

Figure 10: *(Panels A-E) Surface brightness maps for a typical high-mass spiral galaxy according to the simulations of Johnston & Bullock (2006). Each panel shows the same 300 kpc ×300 kpc region, but with increasingly faint surface brightness cutoffs of μ_V = 28, 30, 32, 35 and 40 mag arcsec^{-2}, respectively. (Panel E) Surface density map for old, metal-poor stars in M31 based on CFHT imaging from the PAndAS survey (see Richardson et al. 2011). The faintest features visible in this image have $\mu_V \sim$ 33 mag arcsec^{-2}.*

The history of mergers and accretions in luminous galaxies — which are powerful constraints on models of hierarchical galaxy formation — can be examined directly with the resolved stellar populations in their extended halos. Numerical simulations carried out in the framework of CDM models make clear predictions for the number and morphology of satellites, shells, streams and rings in the halos of $z \sim 0$ galaxies. As shown in Figure 10, identifying these halo substructures requires reaching very low surface brightness levels — typically $\mu_V \geq 33$ mag arcsec^{-2}. Such levels can be reached only through direct star counts (rather than surface photometry) and has, in fact, only been achieved in a handful of the nearest galaxies, such as M31 (e.g., McConnachie et al. 2009). With CASTOR, exposure times of ~30 hrs per target would provide 5σ photometry to depths of UV ~ 28, u ~ 29 and g ~ 29, which is adequate to reach below the level of the horizontal branch in old, metal-poor stellar populations at a distance of ~3 Mpc. Dozens of additional galaxies out to the distance of the Virgo cluster could have their upper red giant branches mapped in this way.

3.2. *Structure and Stellar Populations of Halo Substructures*

The Galactic halo contains numerous substructures — or stellar "overdensities" — that can be used to study the history of accretions, star formation and chemical enrichment in the Milky Way (e.g., Tollerud et al. 2011). These include ~160 globular clusters, several prominent stellar streams, and ~2 dozen satellite galaxies (although this number is expected to grow dramatically in the future, thanks to imaging from LSST, Pan-STARRs, Sky-Mapper and even from the CASTOR Wide Survey). Taken together, these substructures hold potentially important information on the low-mass end of the dark matter mass function, as well as on the nature of reionization and feedback in the lowest-mass stellar systems. The key contribution of CASTOR to this field will likely be in the production of deep, wide-field photometric catalogs for stars belonging to these newly discovered systems (either by CASTOR itself or by contemporaneous ground-based surveys). For instance, as HST studies have shown, it is only through high-resolution imaging, particularly in the UV and blue-optical regions, that the distinct stellar populations in these objects can be identified and studied (see Figure 11; see also Piotto 2009). Observations of hot stars (e.g., HB stars, blue stragglers, sdB stars, white dwarfs, AGB manqué stars), in these objects will be especially fruitful with CASTOR.

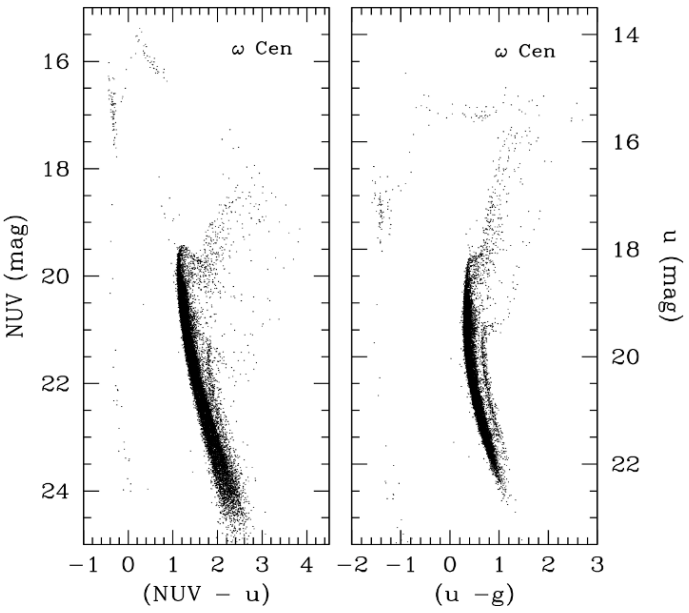

Figure 11: *Color-magnitude diagrams for the Galactic globular cluster ω Cen, based on HST/WFC3 imaging from Bellini et al. (2010). With CASTOR, data of this quality will be possible for several hundred substructures surrounding the Milky Way.*

3.3. White Dwarfs in the Galactic Halo

White dwarfs represents the final evolutionary stage of intermediate-mass stars, when electron degeneracy provides support against gravitational collapse as the star gradually cools. White dwarfs are interesting objects in their own right (e.g., as tests of stellar evolution theory), although they are perhaps most useful as Galactic chronometers. Recently, cool (=old) white dwarfs have also received attention as possible targets of transit searches for planets in the habitable zones of old stars. While much is known about the properties of disk white dwarfs in the local neighborhood, very little is known about white dwarfs in the halo of the Galaxy: i.e., fewer than 50 white dwarfs per deg^2 brighter than g ≈ 24 associated with *any* Galactic component are predicted by Milky Way models (Robin et al. 2003). However, the excellent u-band sensitivity of CASTOR — combined with its ability to perform accurate star-galaxy separation at faint magnitudes by virtue of its HST-like resolution — means that CASTOR will be a powerful probe of Galactic white dwarfs, including those associated with the halo (i.e., located at scale-heights of 5–10 kpc). Indeed, CASTOR will be able to select white dwarfs efficiently from UV-optical color-color diagrams for millions of unresolved sources in the Wide and Deep Surveys.

Some of the most remarkable discoveries to come from HST during the past decade have been the result of its unique capabilities in astrometry, particularly in the measurement of proper motions. Such results include the determination of proper motions (and, hence, orbits) for remote star clusters and satellite galaxies, the possible detection of intermediate-mass black holes in some globular clusters, and the discovery of multiple stellar populations in an ever-increasing number of star clusters after proper motion cleaning of color-magnitude diagrams (Piatek et al. 2007, Andersen & van der Marel 2010, Woodley et al. 2012).

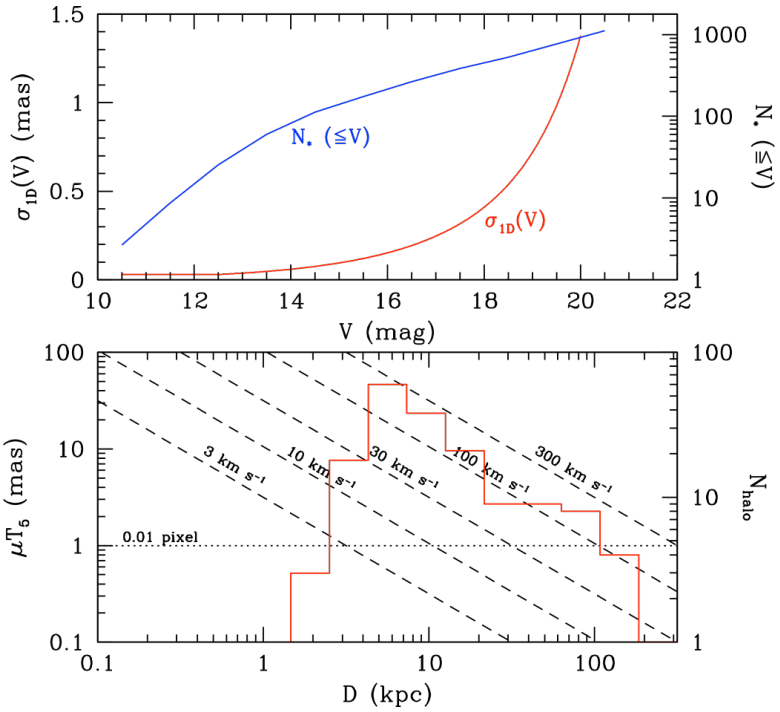

Figure 12: *(Upper Panel) Astrometric precision, 1D(V), for the GAIA all-sky mission as a function of V-band magnitude (red curve). Also shown are the cumulative number of Galactic field stars per CASTOR field, estimated for a high-latitude field using the Besancon models of Robin et al. (2003). (Lower Panel) Positional change over a 5-year baseline, T5, as a function of distance from the Sun for different tangential velocities. The red histogram shows the distance distribution of halo substructures (i.e., globular clusters, dwarf galaxies and ultra-faint dwarfs).*

CASTOR, with its similar image quality but much larger field of view, has the potential to far exceed HST in this area. An important advantage of CASTOR relative to HST, is that, by the end of this decade, ESA's GAIA mission will have established an accurate, all-sky astrometric grid based on positional measurements for roughly one billion Galactic stars (Perryman et al. 2001). As shown in the upper panel of Figure 12, this grid will provide ~1000 "astrometric standards" in each CASTOR field down to GAIA's limiting magnitude of V ≈ 20. Imaging from CASTOR can then be used to measure accurate positions, tied to the GAIA reference frame, for stars with V > 20 (and all GAIA stars brighter than this, subject to saturation constraints). The lower panel of Figure 12 illustrates how repeat observations with CASTOR, separated by a nominal period of 5 years, could be used to measure proper motions and space velocities for star clusters, dwarf galaxies and stellar streams in the halo; for the nearest star clusters, it will also be possible to study their internal dynamics and determine accurate masses for any central black holes. Alternatively, single-epoch data from CASTOR could be combined with archival imaging from HST to give, for many targets, an astrometric baseline of up to a quarter century.

3.4. *The Origin of Compact Stellar Systems*

One of the more pressing questions to have emerged from the study of nearby galaxy clusters during the past decade has been the origin of the faintest and most compact stellar systems. The relationship between these so-called "ultra-compact dwarf" galaxies (UCDs) and massive star clusters remains a mystery, largely because there exists no comprehensive (i.e., complete and unbiased) catalog of star clusters and UCDs within even a single environment. At still lower luminosities, about 20 "ultra-faint dSph galaxies" have been discovered in the Milky Way during the past seven years, prompting efforts to use these galaxies as laboratories for understanding stellar feedback and adiabatic contraction in the lowest-mass dark matter halos. With its excellent sensitivity and superb image quality, CASTOR will allow the first complete and unbiased survey of such compact, low-luminosity objects in the local volume. For instance, a two-week survey of the Virgo cluster, at D ≈ 16.5 Mpc, would allow a complete census of all compact stellar systems down to g ≈ 28 in this environment, equivalent to a limiting stellar mass of roughly $5000 M_{\odot}$. It will also be possible with CASTOR to *resolve* individual UCDs, star clusters and dwarf galaxies with sizes as small as $R_e \approx 3$ pc (0.0125″; Jordán et al. 2005). Such observations would provide a wealth of information (such as luminosities, stellar masses, concentration indices, mean surface densities and spatial distributions) that can be used to tests models for their formation and evolution.

3.5. *Stellar Nuclei in Nearby Galaxies and the Connection to Supermassive Black Holes*

A surprising discovery from several HST surveys undertaken during the past 10–15 years has been detection of compact, structurally distinct stellar components in the centers of most intermediate- and low-mass galaxies. Since these *compact stellar nuclei* are found in galaxies spanning the entire Hubble sequence, and located in a wide diversity of environments, it is clear that a quite generic formation mechanism (or mechanisms) is needed to explain this remarkable ubiquity (Côté et al. 2006, Ferrarese et al. 2006). With its simultaneous wide-field coverage and excellent angular resolution, CASTOR will allow a definitive characterization of the core vs. global structure for complete samples of many thousands of galaxies in field, group and cluster cluster environments. Given the low luminosities of these nuclei (typically less than ~1% of the host galaxy luminosity) and their small sizes ($R_e \leq 0.1''$ at the distance of the Virgo cluster), CASTOR offers the only hope of identifying these nuclei in a complete sample of cluster galaxies, and measuring their luminosities, stellar masses, and structural parameters. Such a survey would certainly be the departure point for future stellar-dynamical studies with 30m-class telescopes that aim to: (1) measure the black hole occupation function in the low-z universe; and (2) characterize the relationship between stellar nuclei and super-massive black holes in $z \sim 0$ galaxies.

4. Stellar Astrophysics

CASTOR offers unique and powerful capabilities in the area of stellar astrophysics by virtue of its wide-field, excellent spatial resolution imaging, UV performance, and spectroscopic capabilities. Figure 8 shows how data from the combined GALEX (NUV) and SDSS (u, g) databases can be used to identify and classify astrophysical sources, including many different types of stars. With CASTOR, it will be possible to use a nearly identical color-color selection but with a spatial resolution ≈ 10 (SDSS) to 30 (GALEX) times better, and with a roughly hundred-fold improvement in depth (e.g., $u_{lim} \approx 22.0$ and 27.1 for SDSS-DR8 and the Wide Survey of CASTOR, respectively). Below, we briefly describe some obvious areas in stellar astrophysics where CASTOR should make important contributions.

4.1. *Hot and Massive Stars*

UV-, u- and g-band imaging from CASTOR would allow efficient isolation of the hottest and most massive stars, with little or no contamination from other sources (see Figure 8). The Wide Survey would allow a complete study of young stellar populations — down to faint limits, in potentially crowded fields and covering 1/8th of the sky — that would be impossible with any other facility. The Nearby Galaxies Survey and the Nearby Clusters Survey will similarly provide deep and homogeneous samples of such stars in the local volume. For instance, 30 minute exposures with CASTOR will go faint enough to reach 9 solar mass, main-sequence (B0) stars in Virgo, and 2 solar mass (A0) main-sequence stars in M31. Slitless spectroscopy for some targets will enable mapping of WR stars in all local group galaxies, subject to crowding limitations. Such global studies of star formation in local environments will be a unique contribution of CASTOR and of considerable importance to the stellar evolutionary community by providing much-needed constraints on high-mass star formation and feedback from stellar winds.

4.2. *Symbiotic Binaries*

The blue outliers in the lower right region of Figure 8 are symbiotic binaries, which have components of similar luminosity but very different temperatures (i.e., binaries in which one star has become a red giant and is transferring mass to a hot, compact companion). To date, such binaries have been discovered entirely serendipitously. CASTOR would enable a global study of this important stage of evolution in nearby galaxies and, for the first time, allow a detailed comparison between observations and the predictions of stellar evolution models. Spectra will be invaluable in separating the components of these rare but important systems.

4.3. *Degenerate Stars in Dense Stellar Systems*

CASTOR will be an efficient tool for identifying and studying the hottest white dwarfs in star clusters. Deep UV-, u- and g-band exposures will greatly extend the pioneering work carried out by HST on Galactic white dwarfs by mapping out white dwarf cooling sequences and measuring cluster ages. In addition,

CASTOR will readily identify other types of "stellar exotica" in star clusters and dwarf satellites, such as cataclysmic variables and sdB stars, and measure their spatial distribution and fundamental parameters (effective temperatures, intrinsic variability, binary light curves) through repeated, short-exposure observations.

4.4. *X-Ray Binaries and Transients*

The spatial resolution and sensitivity of CASTOR will make it ideally suited to identifying the UV/optical counterparts of X-ray sources. Somewhat surprisingly, the global populations of X-ray binaries in Local Group galaxies have not been fully studied despite their significance in understanding star formation as well as the fundamental physics of extreme objects. Such a program would likely consist of new monitoring exposures (to identify previously unknown transients) as well as data taken as part of surveys (i.e., the Nearby Galaxies Survey or Wide Survey). In addition to monitoring X-ray sources, novae, supernovae, and even GRBs, could be followed up by CASTOR. Spectroscopic monitoring will add greatly to the value of this imaging, by locating emission line objects.

4.5. *Pulsating Variables*

Unprecedented studies of pulsating variables in nearby galaxies, such as RR Lyraes and Cepheids, could be carried out with CASTOR. For example, RR Lyraes in Local Group galaxies could be detected with nearly 100% completeness in just ~30 minute exposures. A series of exposures spanning a day or so would be required to identify these variables, whose periods and luminosities would yield an independent determination of the local distance ladder. Such data would also allow an assessment of whether the Oosterhoff dichotomy exists in other environments, a matter of longstanding debate. The same observations used in the search for pulsating variable will also reveal massive eclipsing binaries in nearby galaxies, yielding stellar masses and additional (independent) distance measurements.

4.6. *Post-AGB Stars and Planetary Nebulae*

Post-AGB stars reflect a brief evolutionary phase for stars of a few solar masses, when the star becomes hot, luminous, and variable. The systems are of interest in understanding the final stages of stellar evolution and may be an important source of emission line spectra of LINER galaxies (rather than low-energy AGNs). CASTOR UV monitoring will readily discover such stars in galaxies out to the distance of the Virgo cluster, while CASTOR spectra will also reveal PNe in these galaxies via their characteristic emission-line properties, providing observational constraints on the formation histories of intermediate mass stars.

4.7. *Extremely Metal-Poor Stars*

CASTOR would be the obvious instrument to perform a dedicated, wide-area search for hot stars in the Galactic halo (e.g., through the Wide Survey; see §IIIa). The addition of slitless spectroscopy for a subset of the Wide Survey fields would be powerful resource for the identification of candidate metal-poor stars, for ground-based follow up at high spectral resolution. In combination with imaging in other optical bands (e.g., Euclid, LSST) CASTOR could map structure of the Milky Way halo out to unprecedented radii (see Jurić et al. 2008).

It is worth re-emphasizing that *any* CASTOR exposures will contain a number of Galactic halo stars (e.g., a typical high-latitude CASTOR field in the Wide Survey will contain an average of ~7000 halo stars brighter than g = 27.8). In other words, each of the CASTOR Legacy Surveys, as well as virtually every GO program that might be implemented, would have an enormous potential for stellar/halo studies. In fact, a coordinated spectroscopic survey with large multi-object spectroscopic telescopes on the ground (such as ngCFHT) would have huge benefits in many areas of astronomy and cosmology, including Galactic Archaeology and stellar astrophysics.

5. The Outer Solar System

The Outer Solar System (OSS) extends from roughly the orbit of Neptune (30 AU) out to a few thousand AU. This region — which is known include the centaur population, the Kuiper Belt, the scattering/scattered disk and the inner Oort cloud — has experienced little physical or dynamical evolution over the

last 3 billion years and thus provides a window into the ancient processes of giant planet and planetesimal formation (the building blocks of planets). Two decades of theoretical and observational study of the OSS have provided a wealth of new information about the processes of planet formation.

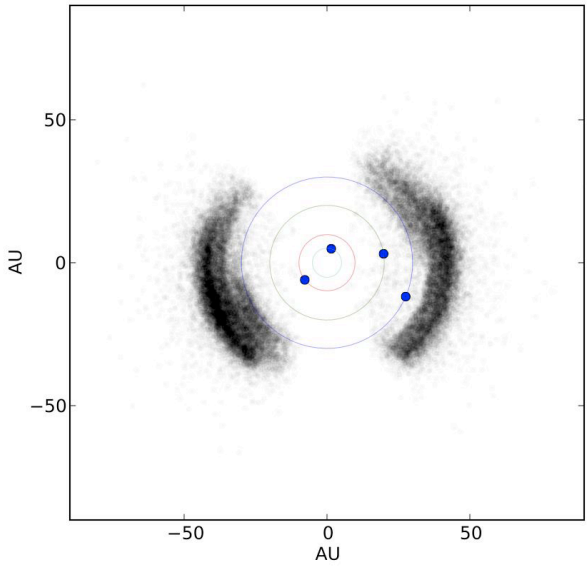

Figure 13: *A top-down view of the outer solar system (OSS). The orbits of the giant planets (Jupiter through Neptune) are shown along with their current locations (blue dots). Grey dots represent the locations of outer solar system objects that will be detected by CASTOR (based on the Canada-France-Ecliptic Plane Survey model of the outer solar system [http://www.cfeps.net]). The 'gaps' in the distribution of OSS objects represents the galactic plane, which will lie outside the CASTOR Wide Survey. Approximately 20000 OSS objects will be discovered during the Wide Survey, a factor of 20 increase in the number of such objects currently known.*

Surveys of the OSS have revealed dynamical complexity and a sometimes puzzling physical structure. The main object classes in the OSS can be grouped according to their current dynamical (orbital) state. The nearest group, the Centaurs, have semi-major axes interior to Neptune as well as high eccentricities. These sources are currently experiencing gravitational scattering with Neptune and will, in a few 10^4 years, become the comets. Beyond Neptune is the Kuiper Belt, which consists of the material with mean orbital radii (i.e., semi-major axes) between 30 and 50 AU. The Kuiper Belt is further composed of a "hot" component whose members exhibit inclined orbits with inclinations in excess of ~2º and a "cold" (or low inclination) component. The "cold" population is yet further sub-structured. Interestingly, the physical properties of these two components of the Kuiper Belt appear distinct. In addition, the "cold" objects are often found in binary systems that are fragile to dynamical perturbation.

Moving beyond the Kuiper Belt one comes to a population of objects whose histories are rather poorly understood, as they shown very large semi-major axes (up to hundreds of AU) and many of these sources appear to be experiencing gravitational encounters with Neptune. These scattering sources are likely objects that were recently ejected from parts of the Kuiper Belt (which is itself only meta-stable) and are transitioning via Neptune encounters to become Centaurs. Finally, stretching beyond these sources one enters the Inner Oort Cloud, whose existence was only established in 2004. The precise origin of this region of the solar system is an area of intense and active research. The emerging picture is that this region of the OSS was formed via gravitational scattering between members of the OSS and stars that formed near the Sun.

However, at this time only two, or perhaps three, members of the OSS population are known, providing few constraints on models of the formation environment of the Sun. Given the small number of known objects the precise boundary between this population and the scattering objects is open to debate; many authors choose to only consider those sources whose closest approach to the Sun is larger than 47 AU as members of the Inner Oort Cloud. At present, roughly 1500 OSS objects are known, of the more than ~10^5 whose detection should be possible and the more than ~10^6 that are thought to exist in this region. Efforts to provide a better measure of the contents of the OSS now dominate the observational landscape in OSS research.

The current flurry of discovery of planetary system and stellar dust rings has clearly demonstrated that many of our previously accepted scenarios of the processes of planet formation must be incomplete. Modern theories of planet formation must explain giant planet systems with orbits of only a few hours duration to ones at distances of hundreds of AU from their host stars. The bewildering variety of planetary systems clearly point to a highly dynamically active phase for those systems and there is no reason to expect that a similar phase did not occur in our own planetary system. Such a dynamically excited phase for our solar system would have imprinted its signature on the structure of the small body belts (i.e., the asteroid and Kuiper Belts, and the Inner Oort Cloud), placing objects in the small body belt reservoirs onto orbits for which the current structure of the solar system provides no reasonable dynamical pathways.

Disentangling the various formation scenarios for the OSS will require a statistically significant sampling of the various subcomponents of the belt. Models that form the Sun in a dense cluster environment (as opposed to a loosely bound open cluster) produce Inner Oort Clouds with different radial distributions; those difference, though, will requires tens of sources with q > 100 AU to be detectable. The process of giant planet migration causes significant stirring of the Kuiper Belt region, effectively disrupting the binary systems with moderately close encounters. A census that includes a large number of KBOs in a range of distance could determine the extent of Neptune‘s past outward motion. More recently, several pieces of evidence appear to point to planetesimals having formed with large sizes. Such a scenario could be tested by examining the size distribution of KBOs down to km-scale objects. Observational surveys of the structure of the OSS will provide important and exciting clues to the solar system‘s formation history; resulting models will help guide our interpretation of data for exoplanetary systems.

The CASTOR Wide Survey will detect more than ~20000 OSS objects, a factor of nearly twenty improvement over existing catalogs (see Figure 13). Although the cadence of the main surveys will provide only limited orbital information, the net knowledge gain for planet formation will be dramatic.

5.1. *Mapping the Inner Oort Cloud*

The lack of known objects with pericenters larger than 47 AU (only two such objects are currently known) leaves an enormous void in our understanding of the evolution of the OSS and the environment in which the Sun formed. Studying the OSS will unveil the formation environment of the Sun (i.e., the nature of the birth cluster), the possible source of Halley-type comets, and the evolution of the giant planet orbits which are themselves coupled to the process of planet formation. The OSS presents the most accessible laboratory for determining and understanding the details of planet formation and planetary system evolution.

Ground-based facilities will continue to provide powerful data sets that are ideal for dynamical modeling the dynamical structure of the OSS. Large programs conducted on the CFHT, as well as results expected from the LSST and PanSTARSS-2 projects, will result in an large number of objects that can be used in probing the evolutionary history of the giant planets. Such surveys, however, will be fundamentally limited in two distinct ways: (1) Individual ground-based surveys, like the CFHTLS, do not cover sufficient area to be sensitive to rare and distant (> 60 AU) solar system objects[4]; while (2) surveys that cover sufficient area do not have the image quality/cadence required to allow the detection of such distant objects. To detect objects at distances beyond 400 AU requires sensitivity to motion of less than 0.3″ per hour. This is well below the sensitivity of typical large-area surveys, which normally observe at cadences of just one hour and often with image quality worse than 1″. Objects bright enough to be detected ($r < 25$) are exceedingly rare (perhaps as few as 400 over the entire sky). The CASTOR Wide Survey, covering ~5000 deg^2 to a depth of $r \sim 26$ with a cadence of three exposures in one hour and an image quality of FWHM = 0.15″ would result in the detection of ~50 such distant sources. As only two such sources are presently known, this would open an entirely new window on the outer solar system.

5.2. *Serendipitous Stellar Occultations*

The size-frequency distribution (SFD) of Kuiper Belt objects is an excellent probe of the processes of planetesimal formation. Indeed, the Kuiper Belt SFD provides the most pristine sampling of these proc-

[4] At a limiting magnitude of $r \sim 25.5$, these objects have a surface density of about 0.01 per deg^2.

esses available in our solar system. A belt of planetesimals will evolve towards an equilibrium SFD over the full size range if coalitional processing dominates for more than a few 100 Myr. If the material in the belt is self-similar (i.e., strength is independent of size), then the equilibrium SFD is a power-law, $n(r)dr = (r/r_0)^{-q}$, with index $q = 3.5$, regardless of the material strength of the bodies. If, however, the objects are not self-similar, but instead have a size dependent strength, then the SFD will exhibit a "wavy" structure that depends on the strength-size relation of the underlying population and the collision speeds. The object size where the SDF transition occurs also depends on the timing of the collision phase and the intensity of gravitational stirring by nearby planets. Measuring the SDF of the surviving material in the Kuiper Belt will provide a measure of the strengths of the KBOs and the collision environment in which they evolved. The 20000 sources detected by CASTOR will allow an unprecedented measurement of the SFD for OSS objects. Unfortunately, the size of the SFD transition likely occurs in objects that are so small and faint ($r \sim 33$) that it is beyond the reach of any facility that relies in reflected sunlight, including CASTOR.

An additional, exciting possibility is to operate CASTOR in a mode where serendipitous occultations of stars by passing Kuiper Belt and Inner Oort Cloud objects can be detected. This is the only technique that is sensitive to sub-km objects in the OSS, and it clearly requires a space-based observing platform. In recent years, CSA completed a concept study for a dedicated space-based occultation observatory (OCLE-DOCLE) and demonstrated the feasibility of this approach with a dedicated 30 cm telescope. A detector focal plane on CASTOR that is capable of reading 300 sampling regions (ROIs) at 10-20 Hz sample speed, once combined with its large aperture relative to OCLE-DOCLE, would allow the detection of multiple occultations by small (sub-km) Kuiper Belt and Inner Oort Cloud objects.

5.3. *UV Observations of KBOs*

Spectroscopic compositional studies of small bodies have played a critical role in helping piece together the formative history of the solar system. This is particularly well demonstrated in the asteroid belt. Not only have spectra revealed that asteroids are primarily silicate in nature, but observations have revealed hydrous and pyritic alteration features. These startling properties have helped paint a picture in which all the silicate material we currently observe in the terrestrial region was once intimately mixed with water — and possibly other — ices. Violent heating both by accretion as well as radiogenic decay caused the water ice to become liquid long enough for aqueous alteration to occur, and in some cases, sufficiently heat the progenitor silicate materials for serpentization and differentiation of the minerals to occur.

Observational efforts are currently ongoing to repeat this same success in the OSS. Unlike in asteroids, ice is a dominant component in OSS objects. Characterization of these ices remains elusive; even their identification is possible only for water-ice and methane which happen to exhibit deep absorption at near-IR wavelengths. Broadband colors for OSS objects reveal a curvature of their reflectance slope (or color) in the u-band to much more neutral colors than that seen in the optical. This has been interpreted as being caused by organic ice, which exhibits a similar behavior. The shape of this flattening into the UV region is not only a diagnostic of the what surfaces ices may exist, but also of the amount of radiation-induced chemistry the ices have undergone. The coarseness of available data (which are primarily colors) prevents quantitative interpretation of the observations. Of the ~20000 OSS objects detected by CASTOR, roughly 800 will have high high-quality u- and g-band measurements (compared to only 10 for which u-band fluxes are currently available). A further subset of roughly 50-100 objects will be bright enough for spectroscopy with resolution R~50 (depending on their UV fluxes, which are currently unknown). Such a data set will allow us, for the first time, to probe the nature of this curvature. For instance, it would allow us to not only constrain the types of ice that exist in the OSS, but also to explore both the nature of the primordial ices from which that these bodies originated, and the chemical pathways that gave rise to them. Colors from CASTOR would thus become the standard reference catalogue for OSS objects.

IV. Technical Implementation

IVa. Concept Overview

CASTOR is a proposed CSA-led ~1250 kg 'smallSAT'-class space telescope mission (see Figure 14). CASTOR has been designed to meet distinct and far ranging scientific goals by virtue of a simple but innovative design and a flexible operations model. These include characterizing the effects of dark energy on the cosmos, understanding the history of galaxy evolution and star formation, and detecting the most distant objects in our solar system. The spacecraft is designed to be compatible with multiple launchers (i.e., Polar Satellite Launch Vehicle, Falcon 9, etc.) and will operate in a sun-synchronous polar orbit with an altitude between 600 and 800 km.

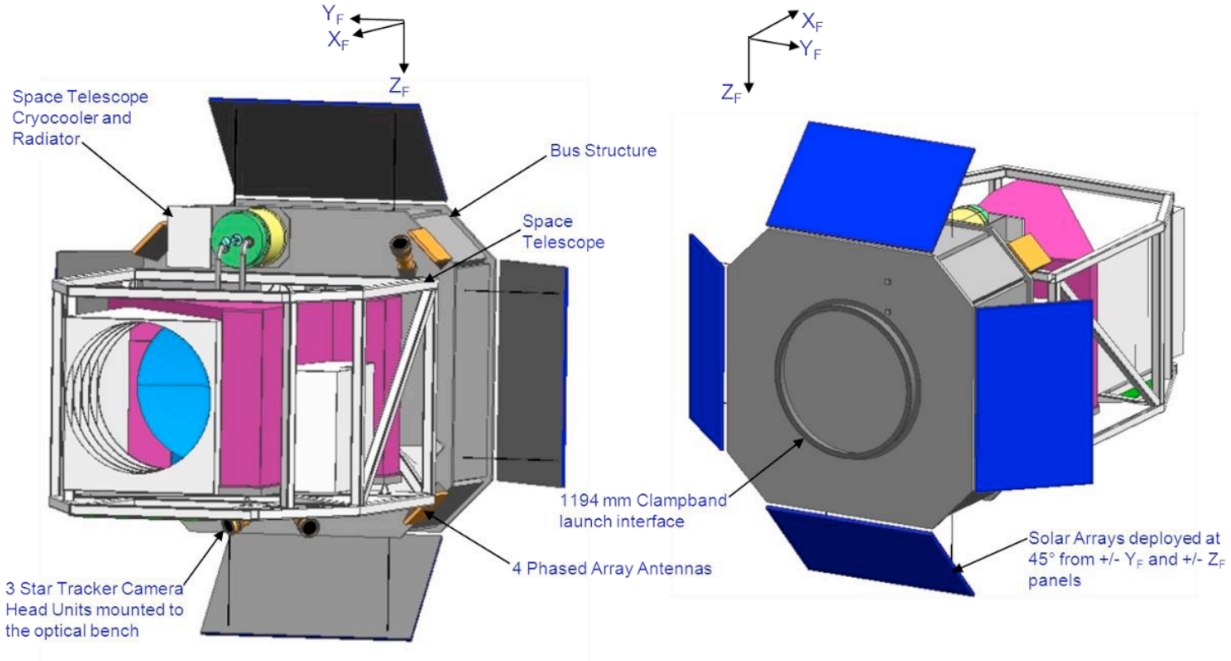

Figure 14: *External spacecraft layout for CASTOR.*

The CASTOR mission features the following fundamental distinguishing capabilities:

- A 1m diameter, unobscured Three Mirror Anastigmat (TMA) telescope that provides Hubble-like image quality of <0.15″ over an unprecedented 1.16° x 0.58° field of view (see Figure 15).
- A huge 725 Megapixel camera with wavelength coverage from 0.15-0.55 μm that allows access to wavelengths that are difficult or impossible to observe from the ground.
- A survey area of 5000 deg^2 in less than 2 years, due to the increased efficiency relative to ground-based telescopes which are limited by daylight and weather to <30% efficiency.
- An unobscured aperture that provides u-band imaging to a depth of > 27 for the Wide Survey. Because high angular resolution leads to improved depth for unresolved sources, CASTOR will have a point source sensitivity comparable to a 40m ground-based telescope in good (0.6″) seeing conditions.

IVb. Payload Layout

The CASTOR instrument consists of the optical assembly, thermal control system, electronics unit and software.

The layout is dictated by the optical prescription with the large input aperture and field of view driving the size of the optical system. The optical path runs through the TMA with its large primary mirror, re-

flecting off the selectable optic on the three axis mechanism, off the fixed fold mirror and onto the Focal Plane Array (FPA). Internal to the TMA, between the secondary and tertiary mirror, is an intermediate image where a shutter mechanism is placed. Another feature of the optical design is an accessible internal pupil, where the three axis mechanism optic resides, this feature is designed in to allow the insertion of a grating for spectroscopy. The optical design includes a fold mirror after the pupil in order to decrease the instrument length for packaging and aid in structural performance.

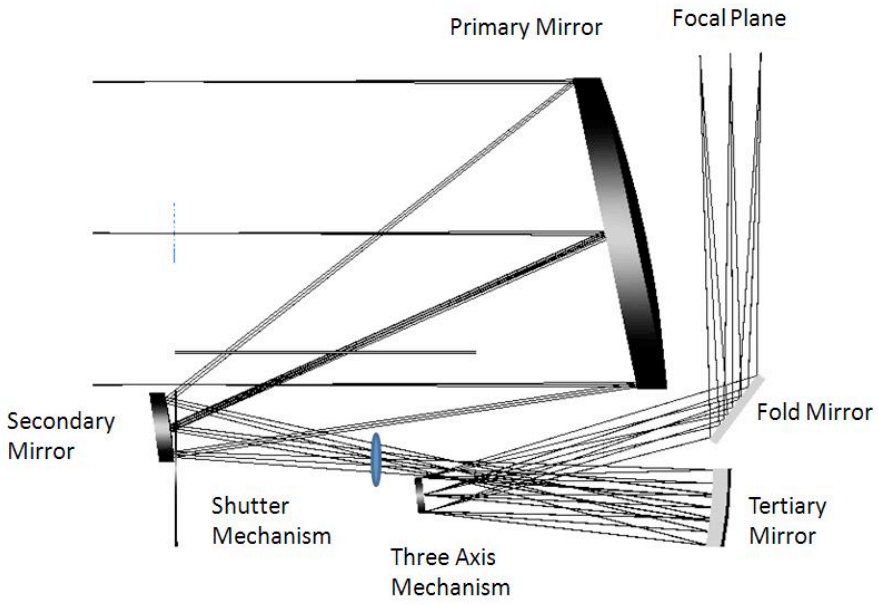

Figure 15: *Telescope optical layout showing the TMA design that delivers a 1.16° x 0.58° field of view with nearly diffraction-limited image quality at* $\lambda < 0.55$ *μm.*

The optical design has the tightest optical tolerances to be located in the TMA assembly. This allows the instrument to be assembled and aligned on the main structure to machining tolerances. The assembly consists of a main structure element, TMA sub-assembly, FPA sub-assembly, three axis mechanism, shutter, contamination cover, fold mirror and kinematic mounts.

The main structure is a composite truss structure with invar or titanium interface mounting pads for attachment of the sub-assemblies and optical components. The interface pads would be designed to allow for shimming or use of a "shoe" for alignment of the optical components. The use of composite material for the main structure is to leverage the high strength to weight ratio as well as low (near zero) CTE to achieve an athermal optical instrument design. Mounting the structure to the bus deck will be done using a kinematic mount design with a large footprint to distribute the loading. The telescope mounting interface will be designed to be vibrationally decoupled from the bus at high frequencies to isolate the imaging function from high frequency momentum wheel jitter, resulting in a reasonably achievable update rate for the fine guidance system.

The TMA is the heart of the telescope design. It is a standalone optical system which will be designed, manufactured, assembled, aligned and tested as a unit. The material for the TMA is SiC, which has exceptional strength to weight and thermal characteristics making the optical system very stable along with providing good optical polishing properties.

The shutter mechanism is located at an intermediate image of the system between the secondary and tertiary mirrors. This feature of the optical design allows for an accessible area to be used as both a shutter system as well as effective stray light control. The shutter will actuated during loss of satellite control or

when the sun may come into view. A one-time deployable door will be used for contamination control during launch and early commissioning of the spacecraft bus.

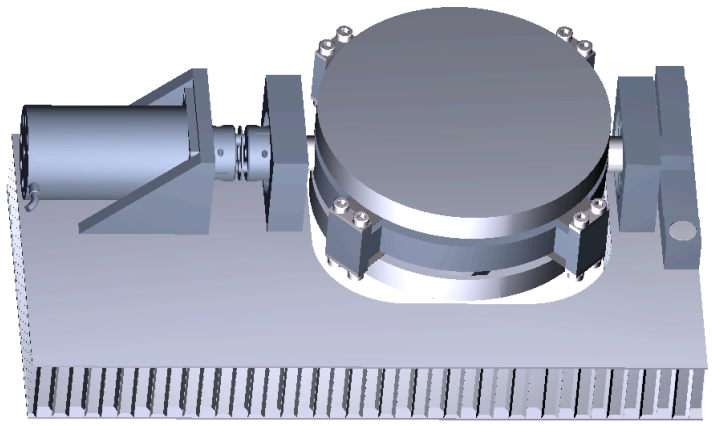

Figure 16: *Conceptual fine steering mirror, showing a two-face, reaction-less tip/tilt system with flip capability.*

A fine steering mirror is placed at the internal pupil of the instrument and will be used for fine alignment while imaging. It will have a turret mount with which two optical elements can be placed and aligned in the optical path (Figure 16). The two selectable optics will be a flat fold mirror for normal mode observing, and a grating for spectroscopy. The mechanism will control tip and tilt of the optic as well as single axis of rotation to select the optic to be placed into the system. It is possible to envision that more faces be added to the turret such that more than one grating, hence spectral resolution be offered. However, the telescope layout would need to be modified slightly to allow more margins between this assembly and the beam passing just above. A flat field calibration source optic could also be added by back illuminating a pot opel diffuser optic when placed in the ray path; the calibration source is currently just a fixed light source inside the telescope enclosure and turned on only during calibration.

A fold mirror is placed and aligned in the system on a mount with a "shoe" interface which allows for alignment on final assembly. The mirror will be fabricated from SiC to maintain the athermal design of the instrument. The mount and interface shoe will be weight-relieved invar to allow for alignment adjustments on assembly.

The FPA consists of the detector array mounted to a SiC assembly plate with cutouts to allow the detector flex cables to feed through and connect to the ASIC readout chips mounted to the back side. The plate will accommodate a thermal strap interface that connects to the cold finger of the cryo-cooler. This thermal strap design will accommodate vibration decoupling from the cryo-cooler pump actuation along with a set of trim heaters and decontamination heaters. Thermal connections will be implemented using heat pipes or thermal straps where appropriate. The FPA assembly plate will be attached to its mount with thermally resistive components to minimize parasitic loads to the FPA cooling system. Detailed design and analysis will be performed to determine an acceptable mounting design which will complement the cooling system analysis.

IVc. Instrument

The driving scientific requirements for the observatory are primarily aimed at conducting a survey using imagery in three bands. The potential to conduct spectroscopic observations once the survey is completed (or sporadically before completion) is viewed as an opportunity of great interest given the near decommissioning of the Hubble Space Telescope and the lack of planned replacement. However, the design philosophy adopted for CASTOR is adding a spectroscopic mode should not affect the likelihood of flying the main mission if significant added complexity and costs were involved. Hence, it was assumed by the design team that the CASTOR should remain a "prime focus" camera-telescope system (Figure 17).

The wavebands, governing the design of the filters and detector coatings are directly based on the scientific requirements:

- A three-channel design for the focal plane is needed for the core science programs discussed in §III: i.e., three "stripes" having filters and coatings optimized to give the highest possible

throughput in UV, u and g bands. Complete coverage over large areas of sky would then be achieved in all bands by stepping and integrating in this layout. Since the latter two bands are "standard" astronomical bands, they should match the commonly defined filters as closely as possible: e.g., the CFHT u band has a central wavelength of 0.374 μm, and a wavelength range at 50% transmission of 0.337−0.411 μm; for the g band, these numbers are 0.487 μm and 0.414−0.559 μm.

- The UV band is defined such that it extends from the cutoff of the u band (the CFHT u filter has 2% transmission at ~ 0.303 μm) as far into the UV as possible, with a requirement of 0.200 μm and a goal of 0.150 μm).

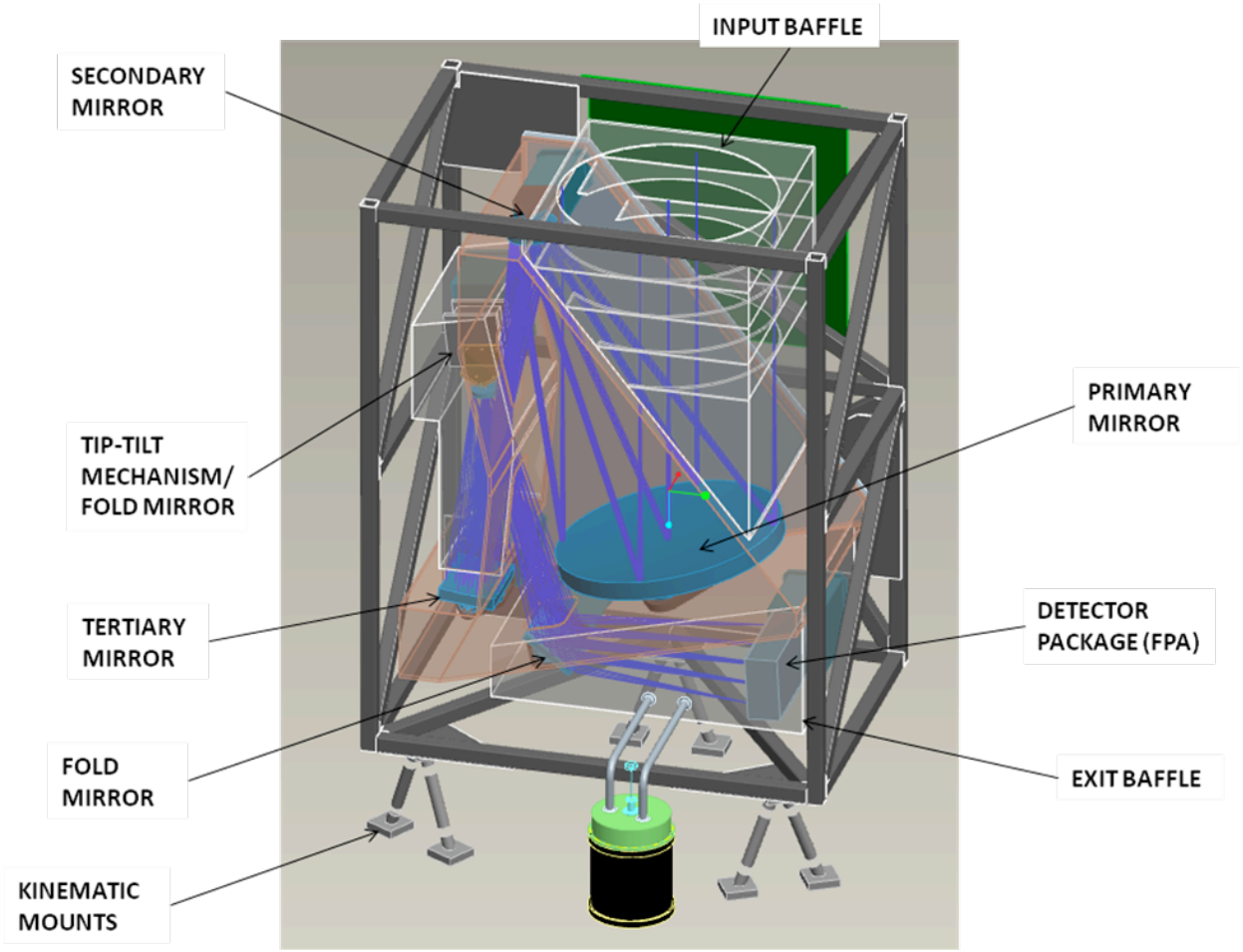

Figure 17: *Payload mechanical layout for CASTOR. The total volume and mass of the payload are 13.8 m^3 and 518 kg, respectively, where the latter value includes a 30% contingency.*

IVd. Detectors

It would ease procurement, qualification, and readout electronics design if the same basic type of detector were to be used for the entire FPA. Detector coatings can vary with little system impact in this case. Detectors are therefore selected to be sensitive over the entire waveband. Silicon based photovoltaic array detectors are known to be highly sensitive over the full spectral range down to 0.12 μm. Suitably mature detector choices include monolithic Back Illuminated CMOS (BICMOS), silicon PIN hybridized to CMOS ROIC (e.g., Teledyne HyVisI), and various flavors of back illuminated CCD (BICCD). "Back illumination" refers to the geometry where light is incident directly on the active area of the silicon, and is

not vignetted by the pixel circuitry and gate contacts as in typical commercial camera chips. This is extremely important for blue and UV sensitivity where the typical photon penetration depth is very small.

With their random access, non-destructive readout capability, random access sub-windowing capability, simplified readout electronics, and intrinsic proton radiation tolerance, we consider CMOS the choice for detectors. An additional advantage is that the Silicon PIN can be hybridized to familiar infrared astronomy ROICs such as the H2RG, recently used by the CSA in the JWST program. One competing drawback, however, is that the PIN material needs extra thickness to retain structural integrity during indium bump bond hybridization (>50 m), and this leads to a larger dark current at fixed operating temperature and higher transient sensitivity to trapped proton flux. CMOS sensors have the additional important operational benefit that many of them support high speed sub-windowing readout without affecting the rest of the scientific data collecting area. This would allow using the main scientific camera as the source for fine guidance information. Indications from Teledyne are that the H4RG-10 will provide less than 0.01 *e/p/s* at around 160 K operating temperature. This will keep the dark current at or below the expected read noise levels on a 10 minute exposure. They have also developed and delivered a 4-side buttable packaging design in collaboration with GL Scientific. This is important for minimizing the gaps between nearby arrays in the FPA. The design allows for <3 mm gaps between active areas of subsequent arrays on 3 sides and <6 mm gap on the fourth bondpad side. The H4RG-10 detectors have been selected as the baseline due to their high TRL, space-qualified status, and mission criticality.

Fine guiding for the fine pointing mirror image stabilizer will be done using small window fast reads in the science array on 2-3 guide stars selected (or recognized) autonomously without interrupting scientific integrations.

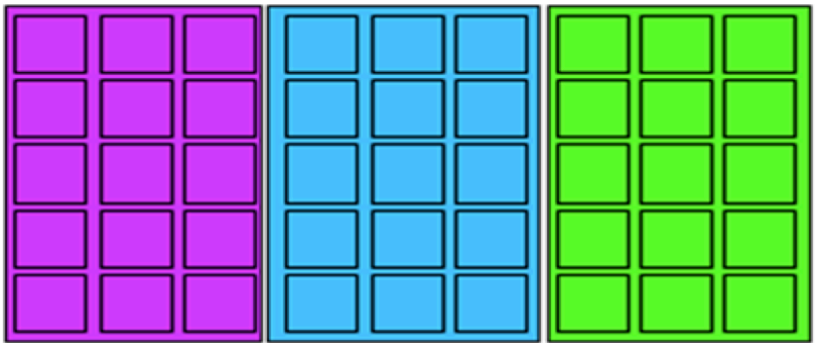

Figure 18: *Proposed focal plane array (FPA) layout for CASTOR, which has a total of 45 4k x 4k detectors. Each band is covered by 3 x 5 FPAs. Gaps between FPAs are neglected in the dimensions shown.*

IVe. Focal Plane Array/ASIC

The FPA identified for this program is the HAWAII-4RG (H4RG). This array is a large (4096×4096 pixel) array with 10 µm pitch (Figure 18). Reference rows and columns are provided for common-mode noise rejection. Guide window output is available with simultaneous science data acquisition of full array. The window is programmable and may be read out at up to 5 MHz pixel rate for guiding. The FPA readout is designed to allow interleaved readout of the guide window and the full frame science data. The FPA provides for a selectable number of outputs (1, 4, 16, 32 or 64) and user-selectable scan directions. The array is 4-side buttable to allow assembly of large mosaics of 4096×4096 H4RG modules, and is fully compatible with the TIS SIDECAR™ ASIC Focal Plane Electronics.

The ASIC back end for the FPA is identical to the version used on the JWST program. The ASIC handles up to 500 kHz A/D conversion with 16-bit resolution per channel, or up to 10 MHz A/D conversion with 12-bit resolution per channel. The ASIC provides a preamp whose gain is programmable from 0dB – 27dB in 3dB steps. There are 32 programmable digital I/O signals (clock generation), 20 programmable bias voltages/currents and a 16-bit fully programmable microcontroller. The ASIC provides 1-24 digital input/output channels for data transfer (LVDS or CMOS).

IVf. Orbit, Launch and Operations

For Earth orbits, sun synchronous LEO orbits are preferred between 600 and 800 km. These allow stable thermal environment and protection of the detectors from solar exposure, stable lighting conditions for astronomy, and modest communications infrastructure. Additionally, these maximize the potential for launch ride sharing. Either a dawn-dusk or dusk-dawn orbit would be targeted depending on launch availability and detailed science objectives. A summary of launch options is given in Table 4.

Table 4. Preliminary Launch Vehicle Survey

Launch Vehicle	Approximate Envelope (mm)	Notes
Delta IV/Atlas V-ESPA	4070 diameter × 6931	Realistic option only if rideshare opportunity is available.
Dnepr	3000 diameter × 5200	Limited quantity based on ICBM, available until ~2020.
Faclcon 1e (2 Stage Burn)	1550 diameter × 1750	Volume too small. Retired, but could be potentially be negotiated with SpaceX.
Falcon 9* (3.6m Fairing)	3200 diameter × 5400	Primary volume could be shared with 1-2 other spacecraft.
Rockot	2100 diameter × 3711	Limited quantity based on ICBM.
Taurus II (Antares) (1.6m Fairing)	1000 diameter × 1828	Volume likely too small.
Minotaur I	1200 diameter × 2100	Currently reserved for US Government payloads.
MinoTaur IV	2000 diameter × 3100+	Currently reserved for US Government payloads.
Pegasus	1100 diameter × 2100	Air launch, may not be in production.
PLSV*	2900 diameter × 4500 (tapered)	Primary volume tight but feasible.
GSLV*	3800 diameter × 6000 (tapered)	Primary volume could be shared with 1-2 other spacecraft.
Ariane 5	4500 diameter × 11500	Realistic option only if rideshare opportunity is available.
Soyuz/Zenit	4000 diameter × 9000	Realistic option only if rideshare opportunity is available.
Vega*	2300 diameter × 5500 (tapered)	Volume potentially too small.

* indicates leading candidate based on availability and cost.

With dawn-dusk or dusk-dawn orbits, there are only short transient eclipses during certain months of the year. Thus a high duty cycle should be achievable. For a duty cycle of 80%, the data generation rate will be roughly seven 10 minute exposures per orbit. Each image will be ~14 gigabits in size, for a total data generation rate of ~100 Gbits per orbit. On board storage and ground links should be designed for 2-3 times this, and data compression may need to be considered. A phased array ground link is very desirable

in eliminating a moving antenna and its associated jitter. Cosmic rays will also be a significant consideration for these orbits and might have an impact for onboard data handling.

With a dawn-dusk or dusk-dawn orbit, scientific surveys will be concentrated in the anti-sun direction, which varies throughout the year relative to the Galactic coordinate system. This implies that most solar panels should be mounted on the anti-sun side, however, in order to survey at some angle off the anti-sun direction (science considerations suggest an off-anti-sun angle of up to 40° would be highly desirable), side mounted solar panels will likely be required.

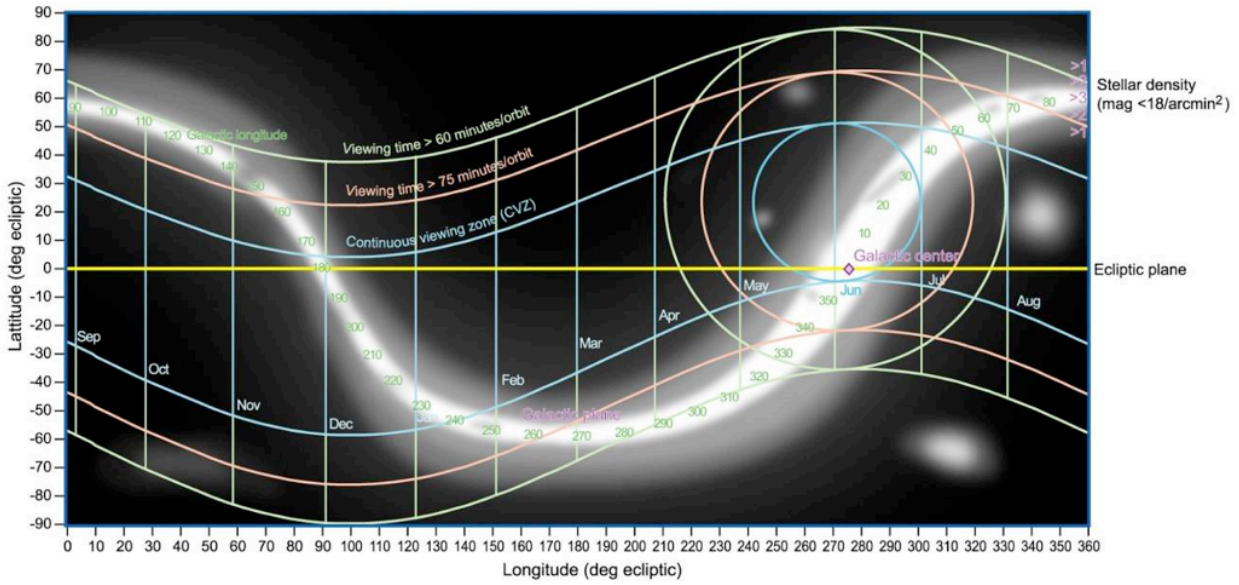

Figure 19: *The monthly variation in the continuous viewing zone (CVZ) for CASTOR is shown by the cyan bands. The orange and green bands show regions with 75-min and 60-min viewing times per orbit for an 800 km sun-synchronous orbit.*

Depending on the time of year, the orbit anti-normal direction will vary between -15.5° and +31.5° away from the anti-Sun direction: i.e. the CVZ is not, in general, centered on the anti-Sun direction, although it is close to anti-Sun direction for much of the year. Figure 19 shows the CVZ throughout the year (as well as 75 minute per orbit and 60 minute per orbit viewing areas) with respect to the Galactic plane. Over the course of the year, the CVZ sweeps out roughly a third of the sky.

While the CASTOR Wide Survey could be carried out entirely within the CVZ, it will be important to conduct deep imaging over intermediate-sized fields (20-40 deg^2) located at, or near, the Galactic poles. The science team has determined that a viewing zone including all regions ~30° from the anti-Sun direction would provide adequate coverage to carry out a wide (5000 deg^2) survey. However, a larger slew from the anti-sun direction would be required for many other science programs (e.g., surveys of M31, the Coma and Fornax clusters, etc). Many of the most interesting extragalactic survey fields are located close to the ecliptic poles (e.g., JWST, Euclid) and it will therefore be important to access these regions, even at the price of reduced observing efficiency. Based on these objectives, the science team has determined that the capability for at least a ±40° slew from the anti-Sun direction is necessary (with a goal of 45°).

A typical mission profile would include imaging within the CVZ at high duty cycle for the majority of the year, with some limited excursions (at lower duty cycle) to areas of interest outside the CVZ at certain times of the year as allowed by power and thermal considerations. The solstices would likely be the best time for these extra-CVZ excursions, since the CVZ will be overlapping with the galactic plane at those times and the spacecraft will be flying over a bright Earth with a lower angle from the terminator to the boresight (reaching a minimum of 25° in December at 800 km).

The data volume budget for CASTOR is summarized in Table 5. The Ground Segment consists of four key systems responsible for controlling, monitoring, and communicating with the space systems, operating the mission, processing and distributing the data, and producing scientific results. The ground station locations should be such that at least one ground station is available for downlink each orbit. As such, international partnerships for science data downlink along with sharing agreements for science data end use should be a key component of CASTOR. The key components of the Ground Segment fulfilling a mission control and/or data processing roles have been considered.

Table 5. Data Volume Budget for CASTOR

Parameters	Values	Units	Notes
Pixels/Exposure	0.725	Giga Pixels/ Exposure	Science team input
Exposures/Image	4	Exposures/Image	Science team input
Time per Exposure	10	Minutes/Exposure	Science team input
Bits per pixel	16	Bits/Pixel	Science team input
Bits per Images	46.4	Giga Bits/Image	
Exposure Time per Image	40	Minutes/Image	Wide Survey
Data Generation Rate	2.4	MB/sec	
Operation duty cycle (Target)	80%		Science team input
Orbital Period	100	Minutes/Orbit	LEO SSO
Data per Orbit	12	GB/orbit	
Data per Day	172.8	GB/day	

Typical scientific operations will start by stabilizing the spacecraft on a target field making up a portion of a legacy survey. During re-pointing operations, the detector arrays will be held in global reset mode to prevent super-saturation damage to the sensitive gate oxides. Once the spacecraft has stabilized to its required levels, the instrument will start imaging. A series of fast images will be taken to acquire a set of guide stars from the known field of view, and determine the position of bright star sub-windows that need to be continuously read out at a high rate to prevent super-saturation. The instrument fine pointing mirror will then be activated to provide fine image stabilization based on the guide star feedback. A series of images will be taken at the appropriate integration time, with multiple non-destructive reads to provide read noise reduction and cosmic ray rejection. This data processing will be done on-board in real time and will be co-added into a final image that will be stored in on-board memory for future download.

Using the proposed CASTOR Wide Survey as a guide, each of the four "dithered" exposures taken at each pointing will be approximately 10 min in duration. Dithering is performed by the instrument to offset the image by half a pixel in the pitch and yaw directions, respectively, in separate images to oversample the PSF. Slightly larger half-integral pixel offsets may be considered to fill in the gaps between individual FPAs.

Because the focal plane array is tiled in three large sections, each optimized for a different passband, the spacecraft will need to yaw or pitch by one third of the field between subsequent images to provide full spectral coverage on each field.

If the optional slitless grating mode is included in the instrument, the fine pointing mirror turret will be designed to be rotated intermittently to replace the planar fine pointing mirror with a slightly curved reflective grating at the pupil stop.

When flat field calibrations are required, the shutter will be closed and an internal UV lamp will be turned on to provide pixel-to-pixel relative photo-response non-uniformity maps. Absolute calibrations across the entire focal plane will be built up over the mission lifetime through statistical brightness measurements on millions of known stars.

The four X-band phased array antennae will be situated such that one will always be pointed at the ground and will be available for science data downlink during ground station overpasses without interrupting science data measurements. This data will then be sent directly to the CADC for processing, archiving, and distribution to the users.

Spacecraft commands and housekeeping telemetry will be transferred using the encrypted S-band link whenever the spacecraft passes over the TT&C stations in St. Hubert or Saskatoon. Most legacy survey science operations will be autonomously generated at the Mission Operations Centre (MOC) in St. Hubert without science team intervention based on the mission plan. Targets of Opportunity and PI-led Science observations will be provided to the MOC for implementation and scheduling through a secure web-based PI interface when appropriate.

V. Education and Public Outreach

The CASTOR mission has the potential not only to transform astronomy, but also to capture the imagination of the public in a way that few scientific projects before it have managed. First and foremost, CASTOR would be an indisputable example of a "flagship" CSA space mission having a high level of international visibility. While HST remains the "gold standard" in terms of public visibility for astronomical facilities, CASTOR could match, or even exceed, HST's high level of visibility, by virtue of its much larger field. Indeed, by combining the wide-field and high-resolution elements of CFHT and HST images that have been so effective in captivating the public, CASTOR would be an unique opportunity for CSA to play a leading role in communicating the importance of science, technology and research to the public. It would also be an extraordinary teaching tool, offering many opportunities for students of all ages to experience the joys of scientific discovery firsthand through outreach programs like Galaxy Zoo[5].

VI. References

Albrecht, A., et al. 2006, e-print arXiv:astro-ph/0609591
Anderson, J.,, & van der Marel, R.P. 2010, ApJ, 710, 1032
Auger, M.W., et al. 2009, ApJ, 705, 1099
Barucci, M.A., et al. 2008, A&A, 477, 665
Bellini, A., et al. 2010, AJ, 140, 631
Benítez, N. 2000, ApJ, 536, 571
Brunetto, R., et al. 2006, Icarus, 180, 546
Bruzual, G., & Charlot, S. 2003, MNRAS, 344, 1000
Cabanac, R.A., et al. 2007, A&A, 461, 813
Conti, A., et al. 2003, AJ, 126, 2330
Côté, P., et al. 2006, ApJ, 165, 57
Cruikshank, D.P., & Dalle Ore, C.M. 2003, Earth, Moon and Planets, 92, 315
Ferrarese, L., et al. 2006, ApJ, 644, L21
Gladders, M.D., & Yee, H.K.C. 2000, AJ, 120, 2148
Hainaut, O.R., & Delsanti, A.C. 2002, A&A, 389, 641
Hildebrandt, H., et al. 2009, A&A, 507, 683
Hildebrandt, H., et al. 2010, A&A, 523, 31
Hildebrandt, H., et al. 2011, ApJ, 733, 30

[5] www.galaxyzoo.org

Hopkins, P., et al. 2010, ApJ, 724, 915
Huterer, D., et al. 2006, MNRAS, 366, 101
Johnston, K.V., et al. 2008, ApJ, 689, 936
Jordán, A., et al. 2005, ApJ, 634, 1002
Jurić, M., et al., 2008, ApJ, 673, 864
Lanzerotti, L.J. 2005, *Assessment of options for extending the life of the Hubble Space Telescope: final report*. Washington, D.C.: National Academies Press.
Leauthaud, A., et al. 2012, ApJ, 744, 159
Martin, D.C., et al. 2005, ApJ, 619, L1
McConnachie et al. 2009, Nature, 461, 66
Milkeraitis, M., et al. 2010, MNRAS, 406, 673
Perryman, M.A.C., et al. 2001, A&A, 369, 339
Piatek, S., et al. 2007, AJ, 133, 818
Piotto, G. 2009, PKAS, 25, 91
Richardson, J.C., et al. 2011, ApJ, 732, 76
Robin, A.C., et al. 2003, A&A, 409, 523
Rozo, E., et al. 2010, ApJ, 708, 645
Sorba, R., & Sawicki, M. 2011, PASP, 123, 777
Tollerud, E.J., et al. 2011, ApJ, 726, 108
Van Waerbeke, L. 2010, MNRAS, 401, 2093
Van Waerbeke, L., et al. 2010, ApJ, 723, 13
Vikhlinin, A., et al. 2009, ApJ, 692, 1060
Welikala, N., & Kneib, J.-P. 2012, eprint arXiv:1202.0494
Wetzel, A.R., Tinker, J.L., & Conroy, C. 2011, eprint arXiv:1107.5311
Woodley, K.A., et al. 2012, AJ, 143, 50